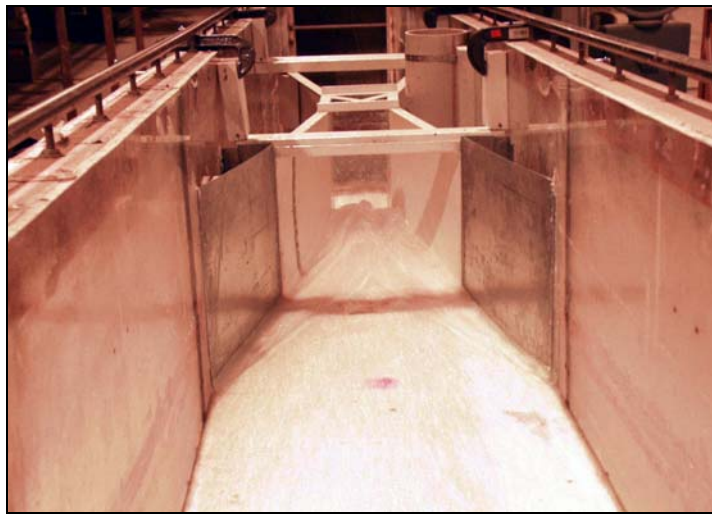


Reese Creek Flume Calibration Study – Phase 2: Parshall Flume Testing

Prepared for:

National Park Service
Water Resources Division
Fort Collins, CO 80525



Prepared by:

Brian A. Smith, Michael D. Robeson,
Christopher I. Thornton (PI), Steven R. Abt (Co-PI)

November 21, 2002

Colorado State University
Engineering Research Center
Fort Collins, CO 80523



Reese Creek Flume Calibration Study – Phase 2: Parshall Flume Testing

Prepared for:

National Park Service
Water Resources Division
Fort Collins, CO 80525

Prepared by:

Brian A. Smith, Michael D. Robeson,
Christopher I. Thornton (PI), Steven R. Abt (Co-PI)

November 21, 2002

Colorado State University
Engineering Research Center
Fort Collins, CO 80523



TABLE OF CONTENTS

1	INTRODUCTION.....	1
1.1	Authorization	2
2	TESTING FACILITY.....	3
2.1	Facility	3
2.2	Flume Modifications.....	4
2.3	Parshall Flume Installation	6
3	TESTING	9
3.1	Introduction.....	9
3.2	Roughness Element Types.....	12
3.2.1	Roughness Type I	12
3.2.2	Roughness Type II.....	13
3.2.3	Roughness Type III.....	14
3.3	Testing Procedures.....	16
4	DATA ANALYSIS	18
4.1	Introduction.....	18
4.2	Database.....	18
4.3	Empirical Equation Development.....	24
4.4	Sensitivity Analysis	38
4.5	Discussion of Results.....	46
4.5.1	Slope Sensitivity Analysis	46
4.5.2	Roughness Sensitivity Analysis.....	50
4.5.3	Flow Regime Observations.....	53
5	CONCLUSIONS AND RECOMMENDATIONS.....	55
5.1	Conclusions.....	55
5.2	Recommendations.....	57
6	REFERENCES.....	58
	APPENDIX A – EXPANDED DATA TABLES.....	60

LIST OF FIGURES

Figure 2.1: Two-foot Flume Prior to Modifications	3
Figure 2.2: Plan View Drawing of False Floor Construction	4
Figure 2.3: Installation of 2x6 Blocks.....	5
Figure 2.4: Completed Installation of False Floor	5
Figure 2.5: Tap and Staff Gauge for h_a Measurement	6
Figure 2.6: Completed Installation of 6-inch Flume.....	7
Figure 2.7: Side View of Testing Flume.....	8
Figure 3.1: Roughness Type I.....	12
Figure 3.2: Roughness Type II.....	13
Figure 3.3: Gradation Curve of Rock used for Roughness Type III.....	14
Figure 3.4: Installation of Rock Bed for Roughness Type III	15
Figure 3.5: Completed Installation of Roughness Type III	15
Figure 3.6: Plan View of Data-collection System and Locations.....	16
Figure 3.7: Data Collection.....	17
Figure 4.1: Dimensions of a Parshall Flume (Bos <i>et al.</i> 1989).....	19
Figure 4.2: Plot of Published Discharge Rating Curves for the 6- and 9-inch Flumes.....	25
Figure 4.3: Discharge Rating Curves for the 6-inch Flume – Roughness Type I (All Slopes).....	27
Figure 4.4: Discharge Rating Curves for the 6-inch Flume – Roughness Type II (All Slopes).....	28
Figure 4.5: Discharge Rating Curves for the 9-inch Flume – Roughness Type I (All Slopes).....	29
Figure 4.6: Discharge Rating Curves for the 9-inch Flume – Roughness Type II (All Slopes).....	30
Figure 4.7: Discharge Rating Curves for the 9-inch Flume – Roughness Type III (All Slopes).....	31

Figure 4.8: Discharge Rating Curves for the 6-inch Flume – 4% Slope (Roughness Types I and II)	32
Figure 4.9: Discharge Rating Curves for the 6-inch Flume – 5% Slope (Roughness Types I and II)	33
Figure 4.10: Discharge Rating Curves for the 6-inch Flume – 7% Slope (Roughness Types I and II).....	34
Figure 4.11: Discharge Rating Curves for the 9-inch Flume – 4% Slope (All Roughness Variations).....	35
Figure 4.12: Discharge Rating Curves for the 9-inch Flume – 5% Slope (All Roughness Variations).....	36
Figure 4.13: Discharge Rating Curves for the 9-inch Flume – 7% Slope (All Roughness Variation)	37

LIST OF TABLES

Table 3.1: Test Matrix.....	10
Table 4.1: Database Variable List and Description	19
Table 4.2: Average Manning’s n Values for Roughness Elements	20
Table 4.3: Database.....	21
Table 4.4: Published Rating Equations for 6- and 9-inch Parshall Flumes	24
Table 4.5: List of Equations Developed from Testing.....	26
Table 4.6: Six-inch Parshall Flume Roughness Type I – Variation in Slope	39
Table 4.7: Six-inch Parshall Flume Roughness Type II – Variation in Slope.....	40
Table 4.8: Nine-inch Parshall Flume Roughness Type I – Variation in Slope.....	40
Table 4.9: Nine-inch Parshall Flume Roughness Type II – Variation in Slope	41
Table 4.10: Nine-inch Parshall Flume Roughness Type III – Variation in Slope	41
Table 4.11: Nine-inch Parshall Flume 4% Slope – Variation in Roughness	43
Table 4.12: Nine-inch Parshall Flume 5% Slope – Variation in Roughness	44
Table 4.13: Nine-inch Parshall Flume 7% Slope – Variation in Roughness	45
Table A.1: Expanded Version of Table 4.6	61
Table A.2: Expanded Version of Table 4.9	61
Table A.3: Expanded Version of Table 4.10	62
Table A.4: Six-inch Parshall Flume 4% Slope – Variation in Roughness.....	63
Table A.5: Six-inch Parshall Flume 5% Slope – Variation in Roughness.....	64
Table A.6: Six-inch Parshall Flume 7% Slope – Variation in Roughness.....	65
Table A.7: Expanded Version of Table 4.11	66
Table A.8: Expanded Version of Table 4.12	67
Table A.9: Expanded Version of Table 4.13	68

1 INTRODUCTION

Reese Creek, located along the northern boundary of Yellowstone National Park, flows into the Yellowstone River downstream of Gardiner, Montana. Currently, the United States is party to a complex water rights agreement involving the waters of Reese Creek. An agreement was signed in July of 1990 distributing the waters of Reese Creek among four users, including the United States. As part of this agreement, the National Park Service (NPS) is obligated to construct and install flow measurement structures at appropriate points along Reese Creek.

One currently utilized measurement structure consists of a Parshall Flume with a five-foot throat width. NPS hydrologists discovered that the rated discharge for given gauge heights within the flume did not agree with the stream gauge discharge measurements taken over a range of flows. After a field visit involving Colorado State University, Engineering Research Center staff, it was hypothesized that the flow entering the flume was in a supercritical state, which the flume was not designed to measure. To aid the NPS with the flow measurement problems in Reese Creek, Colorado State University proposed a three (3) phase research program.

Phase 1, completed in October of 2001, provided a thorough literature review of flow measurement structures in supercritical regimes. Phase 2 consisted of a series of flume experiments to determine the feasibility of calibrating a Parshall flume to accurately predict discharge in a supercritical flow regime. The objectives for Phase 2 are listed below:

1. Determine the feasibility of generating a rating equation for a Parshall flume installed in a supercritical flow regime;
2. Determine the sensitivity of an empirical calibration equation to upstream bed slope; and
3. Determine the sensitivity of an empirical calibration equation to upstream roughness.

Testing for Phase 2 was conducted in an existing two-foot wide flume, located in the Hydraulics Laboratory at the Engineering Research Center (ERC) of Colorado State University (CSU). Six-inch and 9-inch Parshall flumes were tested on three (3) different slopes with varying upstream roughness. Testing yielded a database of six (6) testing configurations and twenty-eight (28) independent tests for a 6-inch flume, and nine (9) testing configurations and fifty-four (54) independent tests for a 9-inch flume. Testing began in mid-November of 2001 and was completed in March of 2002. Contingent on Phase 2, recommendations for Phase 3 will be presented. Subsequent sections encompass information about the testing facility, testing, data analysis, results, conclusions, and recommendations pertaining to the testing program.

1.1 AUTHORIZATION

This testing was authorized under contract with the National Park Service, Water Resources Division. This funding is greatly appreciated.

2 TESTING FACILITY

2.1 FACILITY

Testing was conducted in a two-foot wide, sixty-foot long re-circulating flume. The flume bed slope was adjustable and ranged from horizontal to a slope of ten (10) percent. Discharges were regulated by a seventy-five (75) horsepower, variable speed pump with a maximum discharge capacity of approximately eleven (11) cubic feet per second (cfs). Bed and water surface elevations were taken from a point gauge assembly mounted to a mobile cart that traversed the sides of the flume. Figure 2.1 presents a photograph of the two-foot flume prior to modification.



Figure 2.1: Two-foot Flume Prior to Modifications

2.2 FLUME MODIFICATIONS

A 40'-long test section was constructed upstream of the proposed Parshall flume location. Due to the downward slope of the throated section and the need to install the Parshall flume level, modifications to the two-foot flume were necessary. A 5-inch high false floor was constructed to cover the entire test section. To obtain the 5-inch height, three (3) 2x6s were stacked on top of each other with a one-half inch thick piece of plywood attached to the top of the 2x6s. Three (3) 1-foot sections were attached together by screws and each stack was siliconed to the permanent flume floor in the pattern depicted in Figure 2.2. Figure 2.3 shows a photograph of the installed pattern schematically outlined in Figure 2.2.

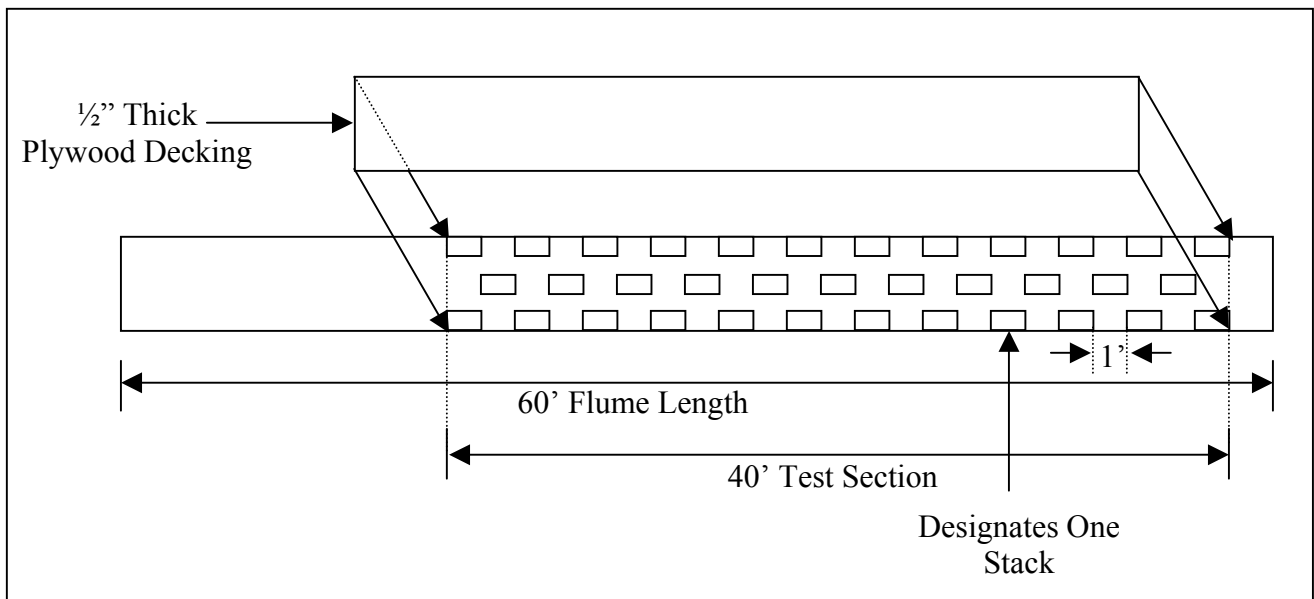


Figure 2.2: Plan View Drawing of False Floor Construction

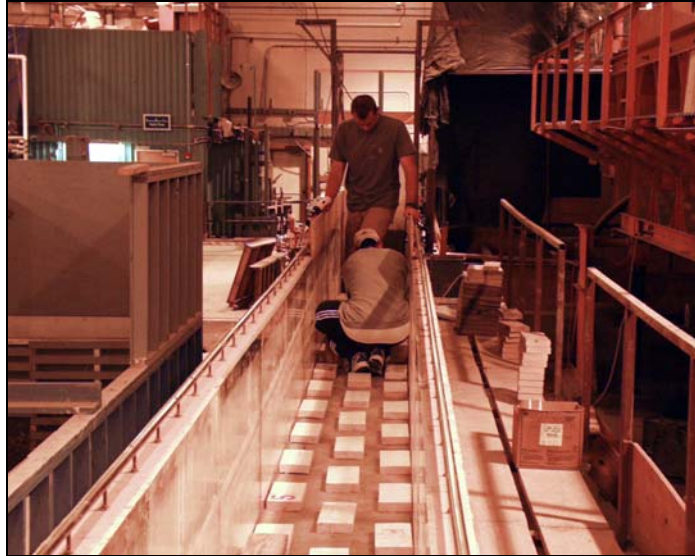


Figure 2.3: Installation of 2x6 Blocks

One-half inch plywood decking was attached to the top of the 2x6 stacks to complete the 5-inch high false floor. An entrance ramp was constructed and put in place to form a transition from the flume floor to the false floor. Figure 2.4 shows a photograph of the completed false floor.



Figure 2.4: Completed Installation of False Floor

2.3 PARSHALL FLUME INSTALLATION

Once the false floor was installed, a 6-inch Parshall flume was placed in the test section. Tests were conducted utilizing both a 6- and 9-inch Parshall flume. A tap was drilled at the appropriate location for the flow depth at a specific location in the flume (h_a) measurement and connected to a stilling well through plastic tubing, thus permitting a conventional measurement of h_a . A staff gauge was also installed on the flume wall opposite of the tap yielding a second method for h_a measurement. Figure 2.5 illustrates the tap and staff gauge used for h_a measurement.



Figure 2.5: Tap and Staff Gauge for h_a Measurement

Shims, composed of wood, steel, and aluminum of varying thickness, were used to bring the Parshall flume entrance to a height even with the false floor. Once even with the false floor,

the downstream side of the Parshall flume was shimmed until the entire flume was level. A standard rod and level were used to level in the Parshall flume at each corner. The Parshall flume was then secured to the 2-foot flume through a system of 2x4s and clamps prior to testing. Wing walls were necessary to converge the flow from the 2-foot wide testing flume down to the approximate 1.30-foot wide entrance of the 6-inch Parshall flume. Wing walls were constructed from sheet metal and installed at the same angle as that of the converging section into the Parshall flume. The 9-inch flume covered nearly the entire 2-foot width of the testing flume making wing walls unnecessary. A photograph of the installed 6-inch Parshall flume is presented in Figure 2.6 and a detailed schematic of the testing flume after completion can be viewed in Figure 2.7.



Figure 2.6: Completed Installation of 6-inch Flume

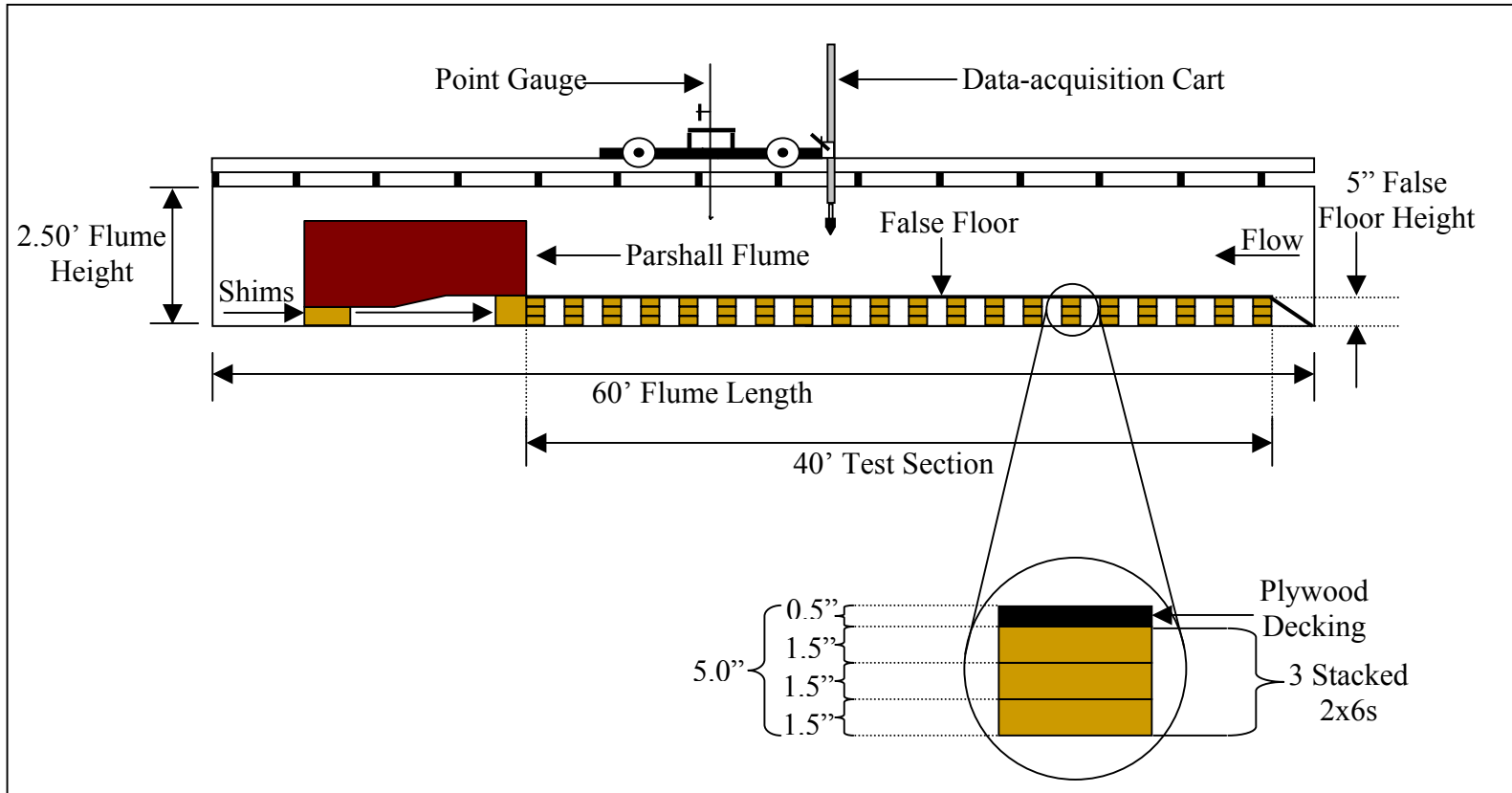


Figure 2.7: Side View of Testing Flume

3 TESTING

3.1 INTRODUCTION

Testing required approximately four (4) months to complete. Fifteen (15) configurations composed of eighty-two (82) independent tests conducted on two Parshall flumes comprise the test matrix. Table 3.1 presents the test matrix, which includes configuration number, test number, Parshall flume size, roughness element type, flume slope, and discharge. Testing was conducted at six (6) different discharges on three (3) separate slopes with three (3) unique upstream roughness elements. For some conditions, however, only four (4) discharges were attainable. The three (3) roughness element types and three (3) slopes utilized during testing were chosen such that an analysis of slope sensitivity and roughness sensitivity to an empirical calibration equation could be conducted.

Table 3.1: Test Matrix

Configuration No.	Test No.	Parshall Flume Size	Roughness Element	Flume Slope	Discharge (ft ³ /s)
1	1	6-inch	Type I	4.00%	1.54
	2	6-inch	Type I	4.00%	2.03
	3	6-inch	Type I	4.00%	2.55
	4	6-inch	Type I	4.00%	3.04
2	5	6-inch	Type I	5.00%	0.97
	6	6-inch	Type I	5.00%	1.47
	7	6-inch	Type I	5.00%	2.01
	8	6-inch	Type I	5.00%	2.53
	9	6-inch	Type I	5.00%	3.05
	10	6-inch	Type I	5.00%	4.06
3	11	6-inch	Type I	7.00%	1.02
	12	6-inch	Type I	7.00%	1.50
	13	6-inch	Type I	7.00%	2.03
	14	6-inch	Type I	7.00%	2.54
	15	6-inch	Type I	7.00%	3.00
	16	6-inch	Type I	7.00%	4.03
4	17	6-inch	Type II	4.00%	0.99
	18	6-inch	Type II	4.00%	1.58
	19	6-inch	Type II	4.00%	2.02
	20	6-inch	Type II	4.00%	2.56
5	21	6-inch	Type II	5.00%	1.07
	22	6-inch	Type II	5.00%	1.51
	23	6-inch	Type II	5.00%	1.99
	24	6-inch	Type II	5.00%	2.57
6	25	6-inch	Type II	7.00%	0.98
	26	6-inch	Type II	7.00%	1.55
	27	6-inch	Type II	7.00%	2.02
	28	6-inch	Type II	7.00%	2.54
7	29	9-inch	Type I	4.00%	1.02
	30	9-inch	Type I	4.00%	1.53
	31	9-inch	Type I	4.00%	1.97
	32	9-inch	Type I	4.00%	2.54
	33	9-inch	Type I	4.00%	3.01
	34	9-inch	Type I	4.00%	4.02
8	35	9-inch	Type I	5.00%	1.06
	36	9-inch	Type I	5.00%	1.51
	37	9-inch	Type I	5.00%	1.99
	38	9-inch	Type I	5.00%	2.52
	39	9-inch	Type I	5.00%	2.98
	40	9-inch	Type I	5.00%	4.01

Table 3.1 (continued):

Configuration No.	Test No.	Parshall Flume Size	Roughness Element	Flume Slope	Discharge (ft³/s)
9	41	9-inch	Type I	7.00%	0.94
	42	9-inch	Type I	7.00%	1.49
	43	9-inch	Type I	7.00%	2.04
	44	9-inch	Type I	7.00%	2.55
	45	9-inch	Type I	7.00%	2.99
	46	9-inch	Type I	7.00%	4.02
10	47	9-inch	Type II	4.00%	1.06
	48	9-inch	Type II	4.00%	1.48
	49	9-inch	Type II	4.00%	1.96
	50	9-inch	Type II	4.00%	2.55
	51	9-inch	Type II	4.00%	2.97
	52	9-inch	Type II	4.00%	4.05
11	53	9-inch	Type II	5.00%	0.98
	54	9-inch	Type II	5.00%	1.52
	55	9-inch	Type II	5.00%	2.01
	56	9-inch	Type II	5.00%	2.51
	57	9-inch	Type II	5.00%	2.97
	58	9-inch	Type II	5.00%	4.03
12	59	9-inch	Type II	7.00%	0.97
	60	9-inch	Type II	7.00%	1.49
	61	9-inch	Type II	7.00%	2.02
	62	9-inch	Type II	7.00%	2.53
	63	9-inch	Type II	7.00%	2.97
	64	9-inch	Type II	7.00%	4.06
13	65	9-inch	Type III	4.00%	0.98
	66	9-inch	Type III	4.00%	1.48
	67	9-inch	Type III	4.00%	1.99
	68	9-inch	Type III	4.00%	2.49
	69	9-inch	Type III	4.00%	3.02
	70	9-inch	Type III	4.00%	4.03
14	71	9-inch	Type III	5.00%	0.98
	72	9-inch	Type III	5.00%	1.50
	73	9-inch	Type III	5.00%	1.99
	74	9-inch	Type III	5.00%	2.52
	75	9-inch	Type III	5.00%	3.01
	76	9-inch	Type III	5.00%	4.03
15	77	9-inch	Type III	7.00%	0.98
	78	9-inch	Type III	7.00%	1.50
	79	9-inch	Type III	7.00%	2.03
	80	9-inch	Type III	7.00%	2.51
	81	9-inch	Type III	7.00%	2.98
	82	9-inch	Type III	7.00%	3.98

3.2 ROUGHNESS ELEMENT TYPES

Three (3) separate roughness element types were incorporated into the testing program and designated as Type I, Type II, and Type III. Types I and II were utilized for testing with both the 6- and 9-inch Parshall flumes. Type III was only tested in conjunction with the 9-inch Parshall flume. Descriptions of the installation procedures for each roughness type are given in the following sections.

3.2.1 ROUGHNESS TYPE I

The smooth, plywood false floor itself was utilized for roughness element Type I. Section 2.2 of this report describes the installation procedures of the plywood decking while Figure 3.1 shows a photograph of the plywood used for roughness Type I.



Figure 3.1: Roughness Type I

3.2.2 ROUGHNESS TYPE II

The roughness of Type II was increased in comparison to that of Type I. AstroTurf® was chosen as an appropriate roughness element for roughness Type II. Prior to installation, 2-foot wide strips of AstroTurf® were cut to fit the floor of the testing flume. Once cut, the AstroTurf® was attached to the plywood decking with staples. No particular stapling pattern was followed during AstroTurf® installation, however, the sides and seams where two separate AstroTurf® pieces joined together were heavily stapled to prevent the AstroTurf® from lifting. Prior to testing, flow was conveyed over the AstroTurf® to ensure that lifting of the AstroTurf® and creation of pockets under the AstroTurf® was minimized. Figure 3.2 presents a photograph of roughness Type II installed in the testing flume.



Figure 3.2: Roughness Type II

3.2.3 ROUGHNESS TYPE III

Roughness Type III was composed of gravel and small cobbles. Due to the necessity of gluing the rocks down to make them immobile, a new, unpainted plywood decking was constructed. The new 1/4-inch thick plywood decking was cut to fit the width of the testing flume and was glued to the old plywood decking. A pebble count was conducted to determine the gradation of the rock used for testing. Individual rocks were randomly spread out to simulate the bed of a gravel/cobble stream. One-hundred (100) rocks were picked at random and particle size was determined using square hole templates ranging in sizes from 1.25 to 6 inches. From the gathered data, it was determined that the d_{50} of the rock utilized for testing was approximately 2.48 inches. A gradation curve produced from the gathered data is presented in Figure 3.3.

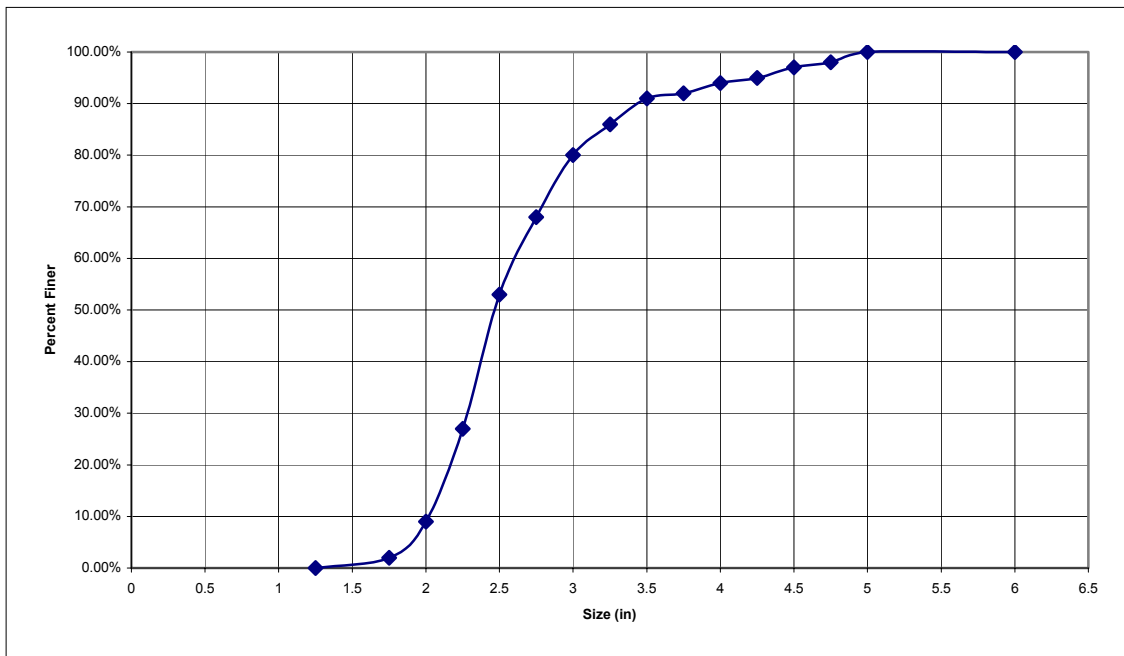


Figure 3.3: Gradation Curve of Rock used for Roughness Type III

Rocks were randomly selected for installation on the plywood decking. Each rock was dipped in construction adhesive and hand placed on the 1/4-inch plywood. Construction adhesive was used to ensure that the bed would remain immobile during testing. Once the entire testing section was covered with rock, testing was initiated. Figures 3.4 and 3.5 illustrate the installation process and completed installation of the rock bed, respectively.



Figure 3.4: Installation of Rock Bed for Roughness Type III



Figure 3.5: Completed Installation of Roughness Type III

3.3 TESTING PROCEDURES

The 40-foot test section was broken down into increments for data-collection purposes. Data were not collected in the initial 5.5 feet of the test section as flow was in transition between the flume floor and false floor. Consequently, data were only recorded over 34.5-foot test section downstream of the flume entrance. Data were collected every four (4) feet for the first twenty-eight (28) feet and every two (2) for the next six (6) feet with the twelfth data point being collected directly upstream of the entrance to the Parshall flume. This data-collection system allowed data to be collected at thirteen (13) different cross sections along the section. Figure 3.6 displays the locations where data were collected.

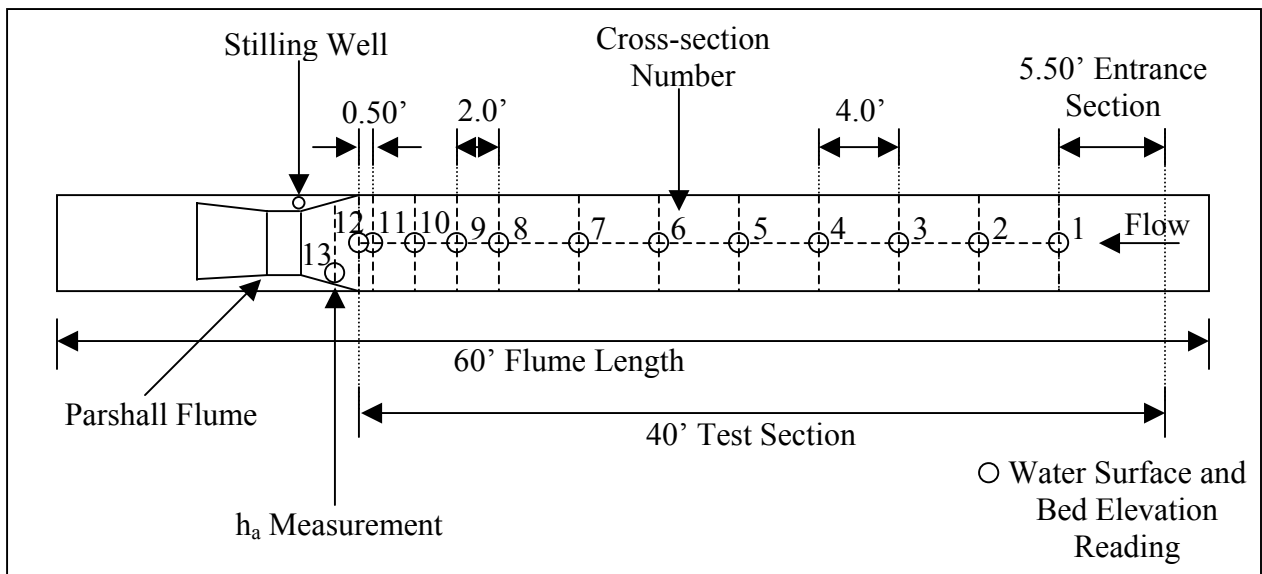


Figure 3.6: Plan View of Data-collection System and Locations

Prior to flow initiation, the appropriate predetermined flume slope was set. Flume slopes were checked and verified by surveying the upstream- and downstream-most points of the test section. When the appropriate flume slope had been reached, the Parshall flume was shimmed and leveled. Bed elevation measurements were recorded at the centerline of each cross section

utilizing an existing point gauge assembly. Once completed, discharge was initiated, increased to the desired flow rate, and allowed to reach equilibrium. Water surface elevations were then recorded with the point gauge in the same locations as the bed elevations to allow for flow depth calculations. Flow depths were insufficient to allow for accurate velocity readings with a 1-D magnetic flow meter, hence, no velocity readings were recorded. General observational data, digital video, and digital still photography were also recorded for each run.

Measurements of h_a were recorded three (3) different ways for comparison purposes. A staff gauge installed on the left side of each Parshall flume allowed for one of the quantifications of h_a . The second method required the recording of a bed and water surface elevation with the point gauge at the h_a measurement cross section, and the third method was to determine h_a from a stilling well measurement. Data collection was held constant throughout all testing and was transferred to a database for analysis purposes. Figure 3.7 presents a photograph of a water surface measurement at the cross section directly upstream of the Parshall flume.



Figure 3.7: Data Collection

4 DATA ANALYSIS

4.1 INTRODUCTION

Upon completion of testing, all recorded data were transferred to a database for analysis. Once all data were organized within the database, analysis procedures were initiated. Subsequent sections discuss and present the variables contained within the database, how these variables were utilized for the development of empirical calibration equations, the sensitivity analysis performed upon the developed empirical rating equations, and finally a discussion of the data analysis results.

4.2 DATABASE

Several hydraulic variables were recorded and considered for input into the database for analysis. After numerous discussions involving the study research team of Dr. Christopher I. Thornton (Principal Investigator) and Dr. Steven R. Abt (Co-Principal Investigator), as well as Mr. Michael D. Robeson and Mr. Brian A. Smith, a list of variables describing the physical processes of the experiment was produced. Table 4.1 presents and describes each variable presented in the database. For illustration purposes, Figure 4.1 provides a schematic of a Parshall flume. All variables included in the database for analysis are located in Table 4.2.

Table 4.1: Database Variable List and Description

Variable	Description
Parshall Flume Size	Throat width of Parshall flumes tested. Designated by the dimension "b" in Figure 4.1
Roughness Element	Type of roughness used in testing. Refer to Table 4.2 for more information
S_o	Bed slope of the testing flume as determined by a survey
Q	Flow rate recorded for each individual run in units of cfs
h_a	Flow depth measured at the specified h_a location in Figure 4.1
Control Volume	The cross-section stations over which hydraulic parameters were analyzed
h	Average flow depth of the specified control volume
S_f	Slope of the energy grade line (friction slope) over the control volume
n	Manning's n roughness coefficient as determined from Equation (4.1)

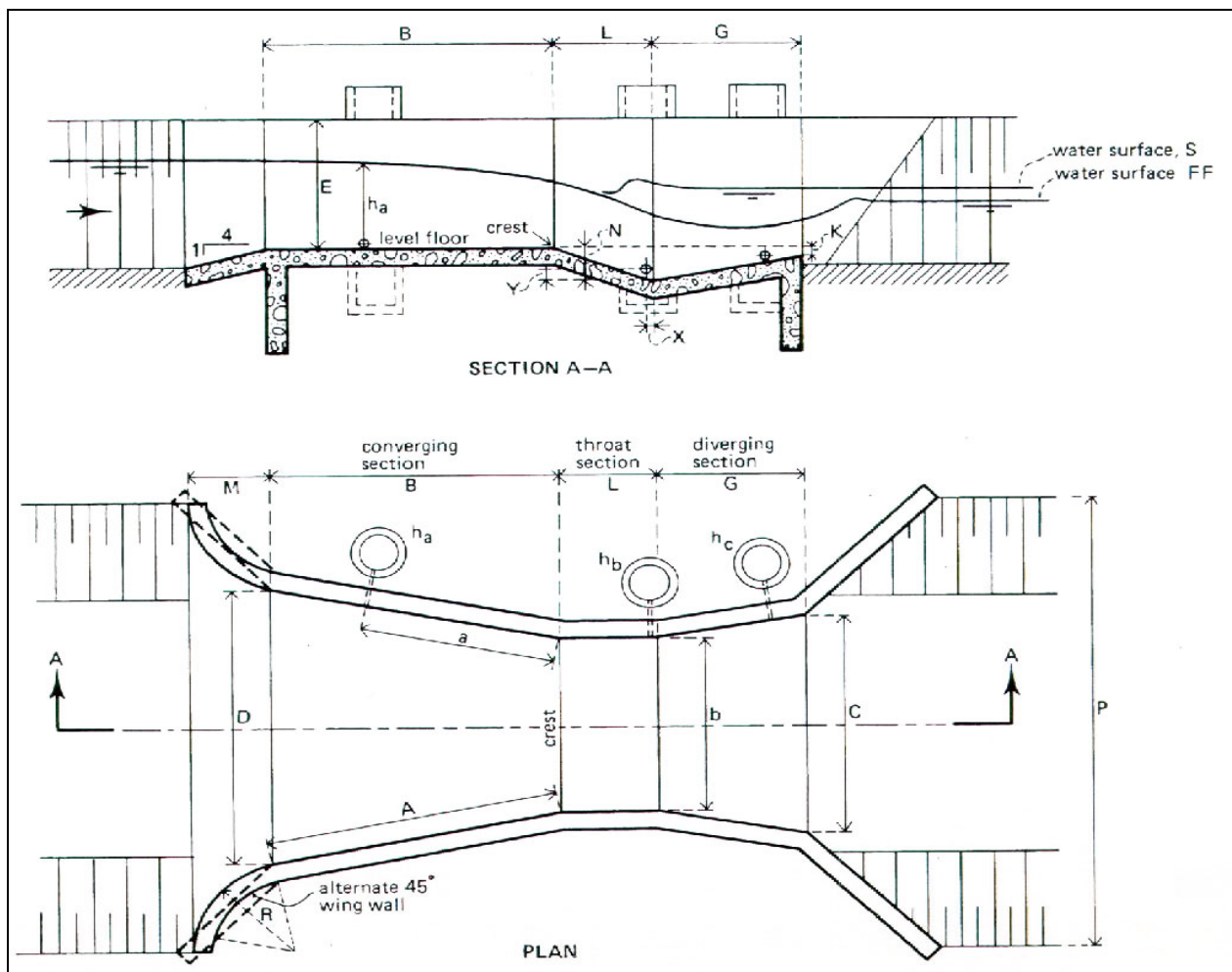


Figure 4.1: Dimensions of a Parshall Flume (Bos *et al.* 1989)

In order to approximate an average Manning’s n value for each roughness type, Manning’s equation (Equation (4.1)) was utilized to compute a roughness coefficient for each of the eighty-two (82) tests conducted in the study.

$$n = \left(\frac{1.486}{Q} \right) A(h)^{2/3} (S_f)^{1/2} \quad \text{Equation (4.1)}$$

where,

- n = Manning’s hydraulic resistance coefficient;
- Q = discharge (ft³/s);
- A = cross-sectional flow area (ft²);
- h = flow depth (ft); and
- S_f = friction slope, or slope of energy grade line (ft/ft).

In Equation (4.1), the flow depth has been used to compute the Manning’s hydraulic resistance coefficient rather than the hydraulic radius. The Plexiglas[®] sidewalls of the 2-foot testing flume were considered hydraulically smooth in comparison to the roughness of the flume bed. Thus, the hydraulic radius variable normally used to compute Manning’s hydraulic resistance coefficient was approximated by the flow depth. All resistance coefficient values computed for each roughness type were then averaged to calculate the mean Manning’s n value for each roughness and are presented in Table 4.2. Table 4.3 presents the database used for the empirical equation development and analysis.

Table 4.2: Average Manning’s n Values for Roughness Elements

Roughness Type	Roughness Description	Average Manning n
Type I	Plywood	0.011
Type II	Astroturf [®]	0.022
Type III	Rock	0.031

Table 4.3: Database

Configu- ration No.	Total Run No.	Individual Test Run No.	Parshall Flume Size	Roughness Element	S_o (ft/ft)	Q (ft³/s)	h_a (ft)	Control Volume	Average Depth h (ft)	S_r (ft/ft)	Approach n
1	1	1	6-inch	Type I	4.00%	1.54	0.230	0-20	0.130	0.04	0.012
	2	2	6-inch	Type I	4.00%	2.03	0.280	0-20	0.162	0.03	0.012
	3	3	6-inch	Type I	4.00%	2.55	0.340	0-20	0.192	0.03	0.012
	4	4	6-inch	Type I	4.00%	3.04	0.390	0-20	0.225	0.03	0.013
2	5	1	6-inch	Type I	5.00%	0.97	0.150	0-20	0.072	0.06	0.009
	6	2	6-inch	Type I	5.00%	1.47	0.190	0-20	0.100	0.05	0.010
	7	3	6-inch	Type I	5.00%	2.01	0.250	0-20	0.147	0.03	0.011
	8	4	6-inch	Type I	5.00%	2.53	0.300	0-20	0.170	0.03	0.011
	9	5	6-inch	Type I	5.00%	3.05	0.350	0-20	0.209	0.03	0.011
	10	6	6-inch	Type I	5.00%	4.06	0.440	0-20	0.267	0.03	0.013
3	11	1	6-inch	Type I	7.00%	1.02	0.150	0-20	0.069	0.06	0.008
	12	2	6-inch	Type I	7.00%	1.50	0.210	0-20	0.099	0.05	0.010
	13	3	6-inch	Type I	7.00%	2.03	0.260	0-20	0.132	0.04	0.010
	14	4	6-inch	Type I	7.00%	2.54	0.320	0-20	0.156	0.04	0.011
	15	5	6-inch	Type I	7.00%	3.00	0.360	0-20	0.186	0.04	0.011
	16	6	6-inch	Type I	7.00%	4.03	0.430	0-20	0.242	0.03	0.013
4	17	1	6-inch	Type II	4.00%	0.99	0.470	0-16	0.119	0.04	0.017
	18	2	6-inch	Type II	4.00%	1.58	0.780	0-16	0.185	0.04	0.022
	19	3	6-inch	Type II	4.00%	2.02	0.930	0-16	0.217	0.04	0.022
	20	4	6-inch	Type II	4.00%	2.56	1.050	0-16	0.246	0.04	0.022
5	21	1	6-inch	Type II	5.00%	1.07	0.490	0-16	0.122	0.05	0.019
	22	2	6-inch	Type II	5.00%	1.51	0.710	0-16	0.164	0.05	0.021
	23	3	6-inch	Type II	5.00%	1.99	0.900	0-16	0.201	0.05	0.022
	24	4	6-inch	Type II	5.00%	2.57	1.050	0-16	0.239	0.05	0.023
6	25	1	6-inch	Type II	7.00%	0.98	0.480	0-16	0.110	0.07	0.020
	26	2	6-inch	Type II	7.00%	1.55	0.780	0-16	0.155	0.07	0.022
	27	3	6-inch	Type II	7.00%	2.02	0.950	0-16	0.188	0.07	0.023
	28	4	6-inch	Type II	7.00%	2.54	1.000	0-16	0.212	0.07	0.022

Table 4.3 (continued):

Configu- ration No.	Total Run No.	Individual Test Run No.	Parshall Flume Size	Roughness Element	S_o (ft/ft)	Q (ft ³ /s)	h_a (ft)	Control Volume	Average Depth h (ft)	S_f (ft/ft)	Approach n
7	29	1	9-inch	Type I	4.00%	1.02	0.160	0-20	0.083	0.03	0.008
	30	2	9-inch	Type I	4.00%	1.53	0.210	0-20	0.126	0.03	0.011
	31	3	9-inch	Type I	4.00%	1.97	0.260	0-20	0.158	0.03	0.012
	32	4	9-inch	Type I	4.00%	2.54	0.300	0-20	0.187	0.03	0.012
	33	5	9-inch	Type I	4.00%	3.01	0.350	0-20	0.217	0.03	0.012
	34	6	9-inch	Type I	4.00%	4.02	0.480	0-20	0.282	0.02	0.013
8	35	1	9-inch	Type I	5.00%	1.06	0.130	0-20	0.071	0.05	0.008
	36	2	9-inch	Type I	5.00%	1.51	0.180	0-20	0.102	0.04	0.009
	37	3	9-inch	Type I	5.00%	1.99	0.250	0-20	0.141	0.04	0.010
	38	4	9-inch	Type I	5.00%	2.52	0.310	0-20	0.169	0.03	0.011
	39	5	9-inch	Type I	5.00%	2.98	0.370	0-20	0.201	0.03	0.012
	40	6	9-inch	Type I	5.00%	4.01	0.440	0-20	0.265	0.03	0.013
9	41	1	9-inch	Type I	7.00%	0.94	0.130	0-20	0.059	0.04	0.005
	42	2	9-inch	Type I	7.00%	1.49	0.180	0-20	0.094	0.04	0.008
	43	3	9-inch	Type I	7.00%	2.04	0.260	0-20	0.130	0.04	0.010
	44	4	9-inch	Type I	7.00%	2.55	0.290	0-20	0.150	0.04	0.009
	45	5	9-inch	Type I	7.00%	2.99	0.330	0-20	0.180	0.03	0.010
	46	6	9-inch	Type I	7.00%	4.02	0.420	0-20	0.236	0.03	0.011
10	47	1	9-inch	Type II	4.00%	1.06	0.370	0-16	0.116	0.04	0.015
	48	2	9-inch	Type II	4.00%	1.48	0.520	0-16	0.161	0.04	0.019
	49	3	9-inch	Type II	4.00%	1.96	0.670	0-16	0.205	0.04	0.021
	50	4	9-inch	Type II	4.00%	2.55	0.810	0-16	0.242	0.04	0.021
	51	5	9-inch	Type II	4.00%	2.97	0.910	0-16	0.274	0.04	0.022
	52	6	9-inch	Type II	4.00%	4.05	1.150	0-16	0.349	0.03	0.023
11	53	1	9-inch	Type II	5.00%	0.98	0.380	0-16	0.120	0.05	0.019
	54	2	9-inch	Type II	5.00%	1.52	0.560	0-16	0.169	0.05	0.022
	55	3	9-inch	Type II	5.00%	2.01	0.700	0-16	0.208	0.05	0.023
	56	4	9-inch	Type II	5.00%	2.51	0.810	0-16	0.243	0.05	0.024
	57	5	9-inch	Type II	5.00%	2.97	0.980	0-16	0.283	0.05	0.026
	58	6	9-inch	Type II	5.00%	4.03	1.190	0-16	0.346	0.04	0.026

Table 4.3 (continued):

Configu- ration No.	Total Run No.	Individual Test Run No.	Parshall Flume Size	Roughness Element	S_o (ft/ft)	Q (ft ³ /s)	h_a (ft)	Control Volume	Average Depth h (ft)	S_f (ft/ft)	Approach n
12	59	1	9-inch	Type II	7.00%	0.97	0.370	0-16	0.107	0.07	0.019
	60	2	9-inch	Type II	7.00%	1.49	0.540	0-16	0.156	0.07	0.023
	61	3	9-inch	Type II	7.00%	2.02	0.270	0-16	0.193	0.07	0.024
	62	4	9-inch	Type II	7.00%	2.53	0.330	0-16	0.226	0.06	0.025
	63	5	9-inch	Type II	7.00%	2.97	0.360	0-16	0.249	0.06	0.024
	64	6	9-inch	Type II	7.00%	4.06	0.460	0-16	0.307	0.06	0.025
13	65	1	9-inch	Type III	4.00%	0.98	0.380	0-20	0.162	0.04	0.029
	66	2	9-inch	Type III	4.00%	1.48	0.580	0-20	0.236	0.04	0.035
	67	3	9-inch	Type III	4.00%	1.99	0.710	0-20	0.286	0.04	0.036
	68	4	9-inch	Type III	4.00%	2.49	0.850	0-20	0.313	0.04	0.033
	69	5	9-inch	Type III	4.00%	3.02	0.990	0-20	0.361	0.04	0.035
	70	6	9-inch	Type III	4.00%	4.03	1.190	0-20	0.426	0.04	0.035
14	71	1	9-inch	Type III	5.00%	0.98	0.350	0-20	0.147	0.05	0.028
	72	2	9-inch	Type III	5.00%	1.50	0.560	0-20	0.208	0.05	0.032
	73	3	9-inch	Type III	5.00%	1.99	0.650	0-20	0.238	0.05	0.030
	74	4	9-inch	Type III	5.00%	2.52	0.770	0-20	0.275	0.05	0.030
	75	5	9-inch	Type III	5.00%	3.01	0.890	0-20	0.309	0.05	0.031
	76	6	9-inch	Type III	5.00%	4.03	1.170	0-20	0.392	0.05	0.034
15	77	1	9-inch	Type III	7.00%	0.98	0.360	0-20	0.119	0.07	0.023
	78	2	9-inch	Type III	7.00%	1.50	0.510	0-20	0.169	0.08	0.028
	79	3	9-inch	Type III	7.00%	2.03	0.650	0-20	0.213	0.07	0.030
	80	4	9-inch	Type III	7.00%	2.51	0.730	0-20	0.245	0.07	0.030
	81	5	9-inch	Type III	7.00%	2.98	0.840	0-20	0.274	0.07	0.031
	82	6	9-inch	Type III	7.00%	3.98	1.130	0-20	0.360	0.07	0.036

4.3 EMPIRICAL EQUATION DEVELOPMENT

The Parshall flume belongs to a general class of open channel water measuring devices known generally as Venturi flumes (U.S. Bureau of Reclamation (USBR) 1984). These devices depend on contraction of the flow either by tapering the sidewalls of the flume, or by changing the elevation of the flume floor, or both (USBR 1984). For any given Parshall flume, each value of discharge (Q) has a corresponding head (h_a) measured from the floor and can be expressed in the following general form:

$$Q = ah_a^b \quad \text{Equation (4.2)}$$

where,

- Q = discharge (ft³/s);
- a = flume geometry coefficient;
- h_a = height of flow measured from flume floor (ft); and
- b = flume geometry exponent.

Published rating equations for the Parshall flumes used throughout the testing program comply with Equation (4.2) and are presented in Table 4.4. Figure 4.2 presents the plot of discharge (Q) versus h_a for the published equations given in Table 4.4. In Figure 4.2, the “Power” equations represent the lines fit to the data utilizing a power equation. Equations presented in Table 4.5 represent power equations fit to the data shown in Figures 4.3 through 4.13.

Table 4.4: Published Rating Equations for 6- and 9-inch Parshall Flumes

Flume Size	Flow Regime	a	b	Equation
6-inch	Subcritical	2.06	1.58	$Q = 2.06h_a^{1.58}$
9-inch	Subcritical	3.07	1.53	$Q = 3.07h_a^{1.53}$

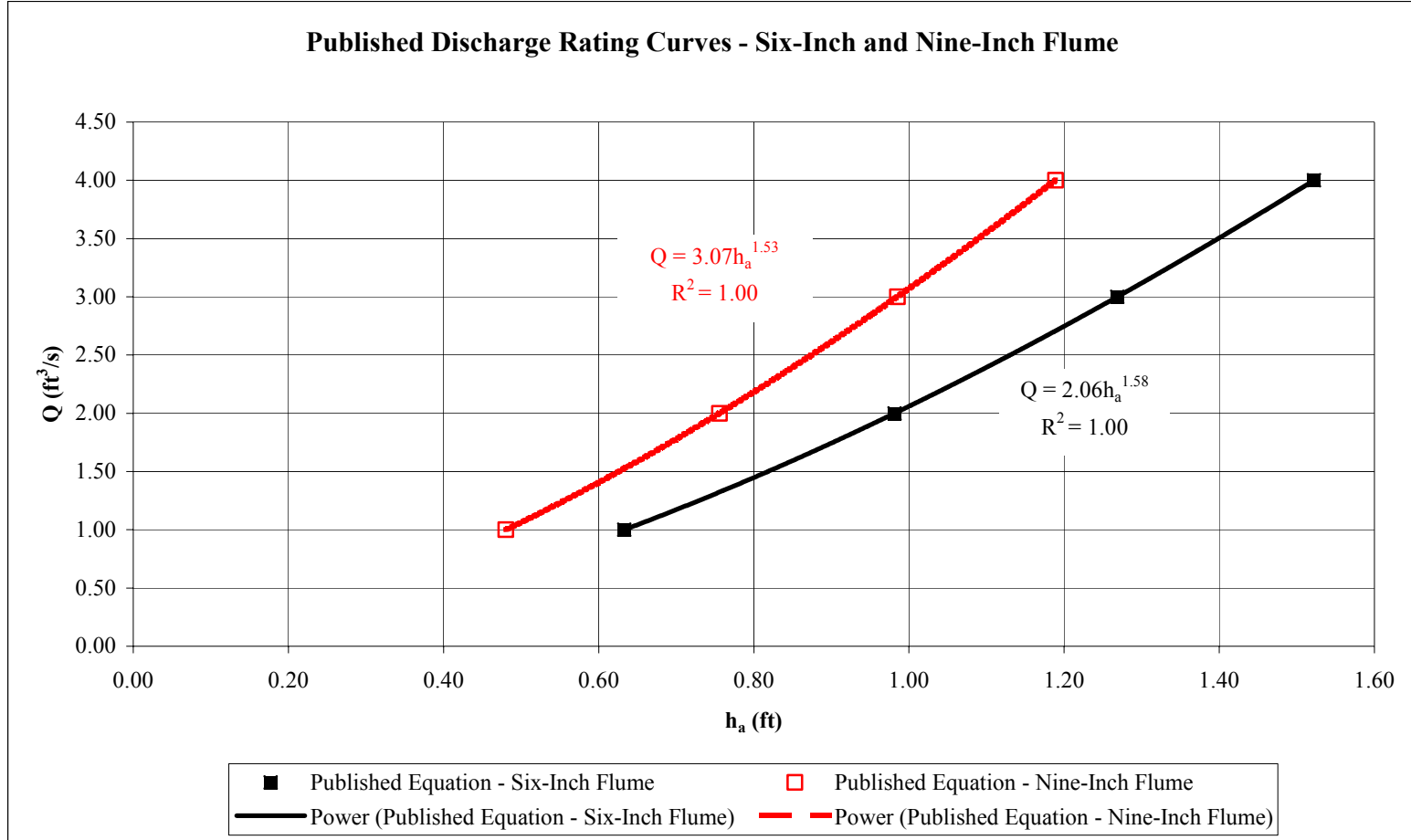


Figure 4.2: Plot of Published Discharge Rating Curves for the 6- and 9-inch Flumes

Table 4.5: List of Equations Developed from Testing

Configu- ration No.	Parshall Flume Size	Rough- ness Type	Slope (%)	Flow Regime	a	b	Equation	Equation No.	
1	6-inch	Type I	4	Supercritical	10.15	1.28	$Q = 10.15h_a^{1.28}$	Equation (4.3)	
2	6-inch	Type I	5	Supercritical	12.00	1.30	$Q = 12.00h_a^{1.30}$	Equation (4.4)	
3	6-inch	Type I	7	Supercritical	11.38	1.28	$Q = 11.38h_a^{1.28}$	Equation (4.5)	
4	6-inch	Type II	4	Subcritical	2.26	1.13	$Q = 2.26h_a^{1.13}$	Equation (4.6)	
5	6-inch	Type II	5	Subcritical	2.32	1.12	$Q = 2.32h_a^{1.12}$	Equation (4.7)	
6	6-inch	Type II	7	Subcritical	2.27	1.19	$Q = 2.27h_a^{1.19}$	Equation (4.8)	
7	9-inch	Type I	4	Supercritical	10.93	1.27	$Q = 10.93h_a^{1.27}$	Equation (4.9)	
8	9-inch	Type I	5	Supercritical	8.79	1.04	$Q = 8.79h_a^{1.04}$	Equation (4.10)	
9	9-inch	Type I	7	Supercritical	11.37	1.22	$Q = 11.37h_a^{1.22}$	Equation (4.11)	
10	9-inch	Type II	4	Subcritical	3.31	1.19	$Q = 3.31h_a^{1.19}$	Equation (4.12)	
11	9-inch	Type II	5	Subcritical	3.16	1.23	$Q = 3.16h_a^{1.23}$	Equation (4.13)	
12	12a	9-inch	Type II	7	Subcritical	3.00	1.14	$Q = 3.00h_a^{1.14}$	Equation (4.14)
	12b	9-inch	Type II	7	Supercritical	11.34	1.33	$Q = 11.34h_a^{1.33}$	Equation (4.15)
13	9-inch	Type III	4	Subcritical	3.09	1.24	$Q = 3.09h_a^{1.24}$	Equation (4.16)	
14	9-inch	Type III	5	Subcritical	3.35	1.21	$Q = 3.35h_a^{1.21}$	Equation (4.17)	
15	9-inch	Type III	7	Subcritical	3.56	1.26	$Q = 3.56h_a^{1.26}$	Equation (4.18)	

According to the USBR (1984), when the values of a and b are determined from actual measurements, the flume can be considered calibrated. The measured variables presented in Table 4.3 were used to develop equations of the general form of Equation (4.2) and are presented in Table 4.5. All of the equations presented in Table 4.5 have a measure of goodness of fit (R^2) greater than 0.95, indicating that at least 95 percent of the variability in the data can be explained with these equations. Due to the fact that the Parshall flume installed in Reese Creek utilizes a direct staff gauge reading for determining h_a , the equations listed in Table 4.5 were computed only from direct staff gauge measurements recorded during testing.

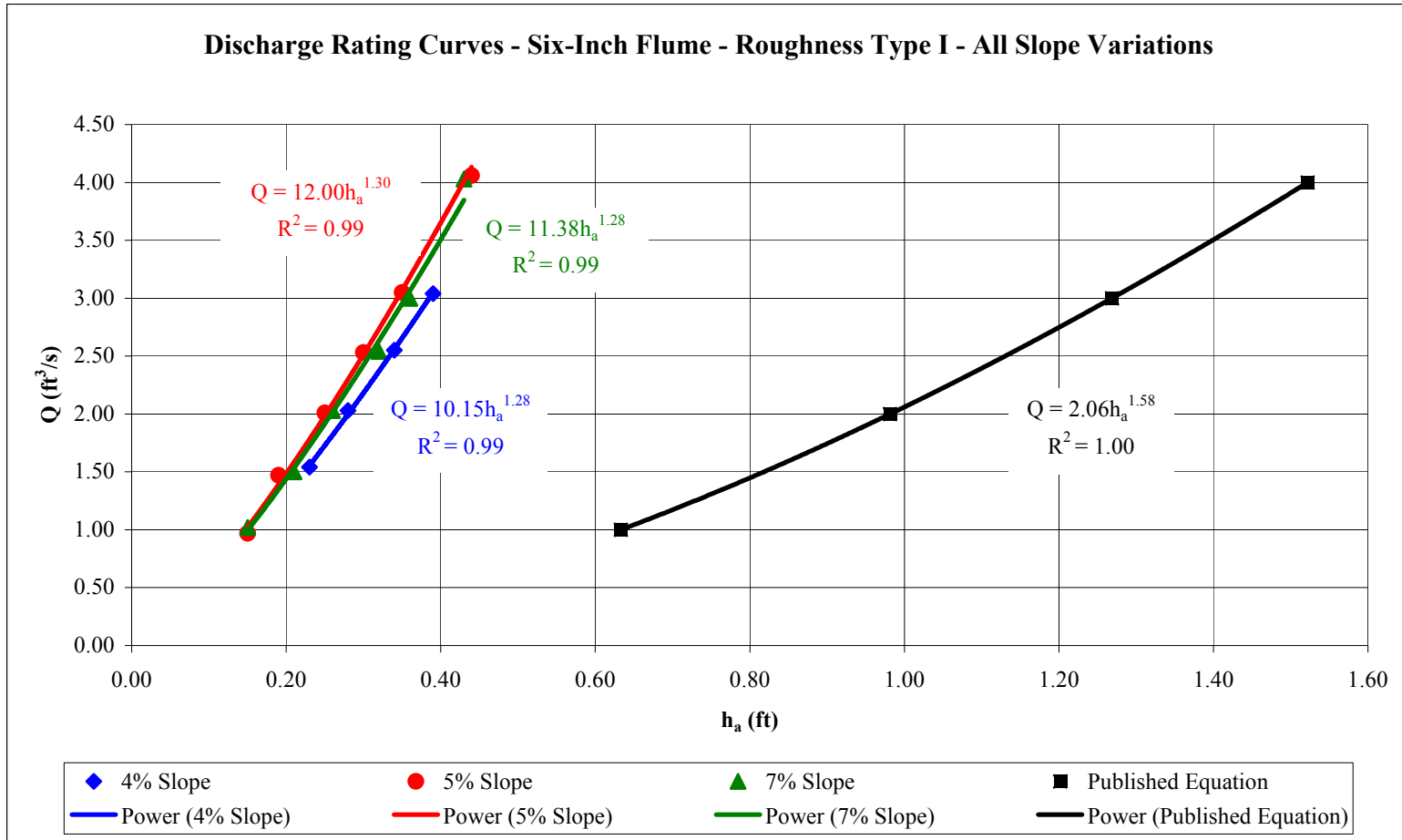


Figure 4.3: Discharge Rating Curves for the 6-inch Flume – Roughness Type I (All Slopes)

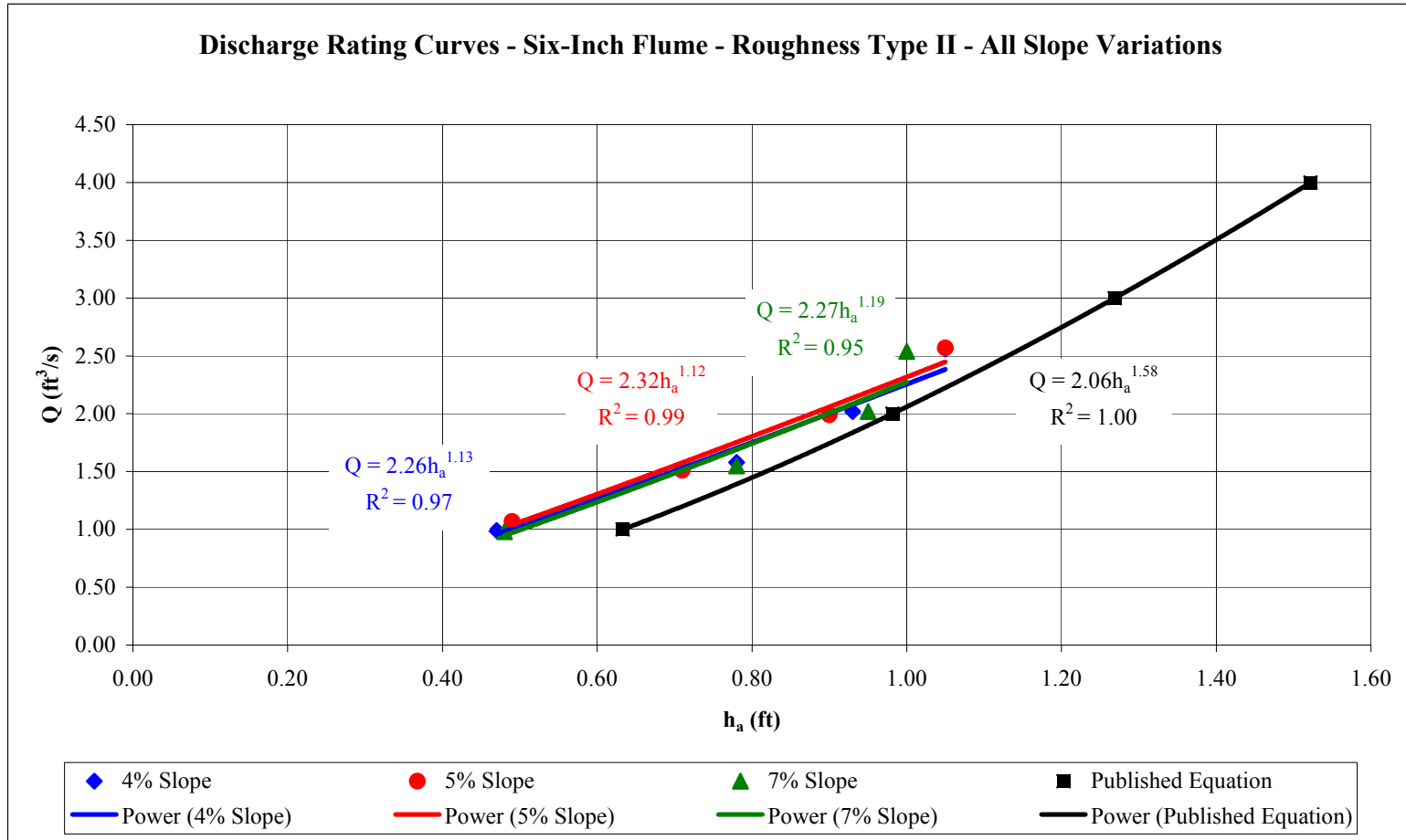


Figure 4.4: Discharge Rating Curves for the 6-inch Flume – Roughness Type II (All Slopes)

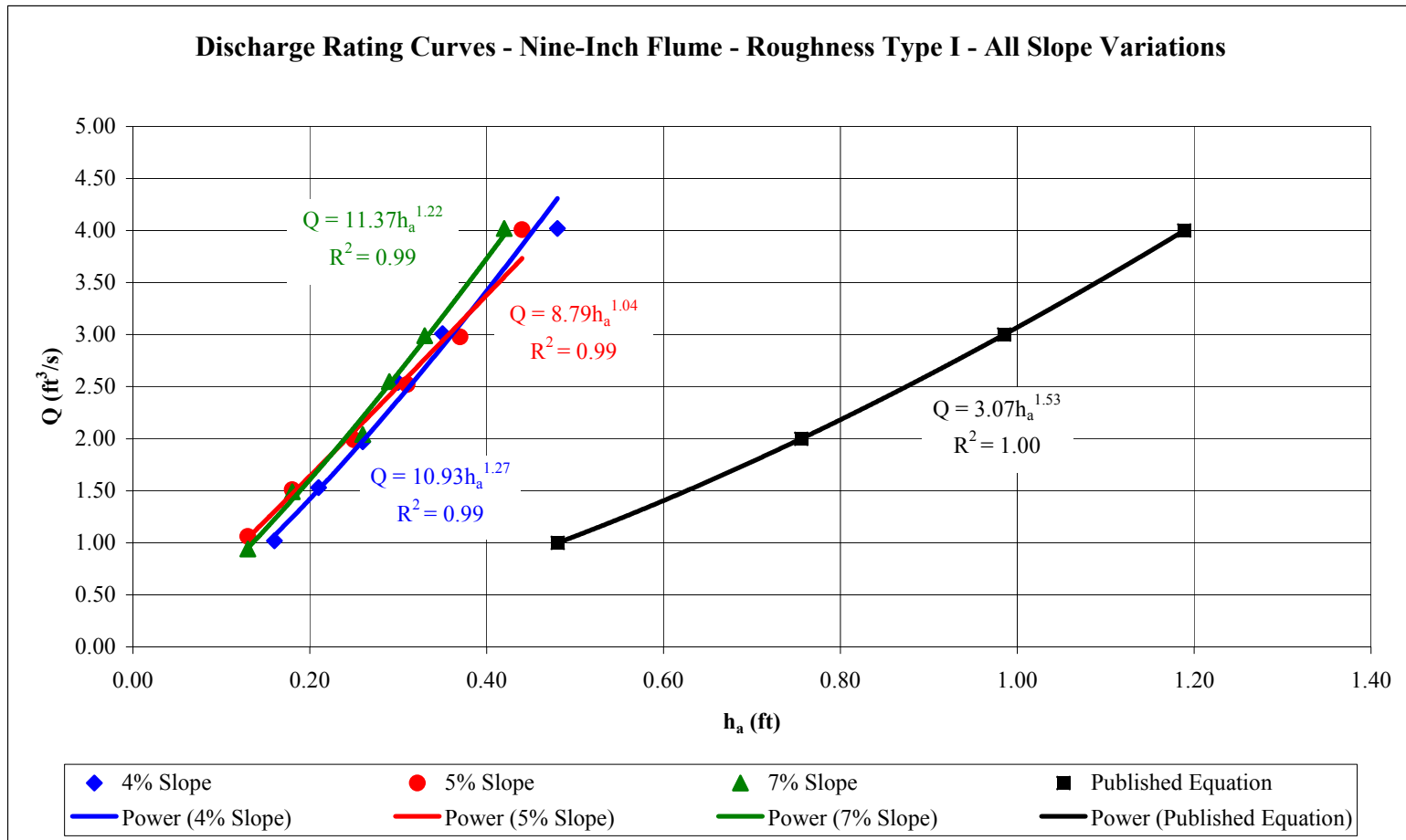


Figure 4.5: Discharge Rating Curves for the 9-inch Flume – Roughness Type I (All Slopes)

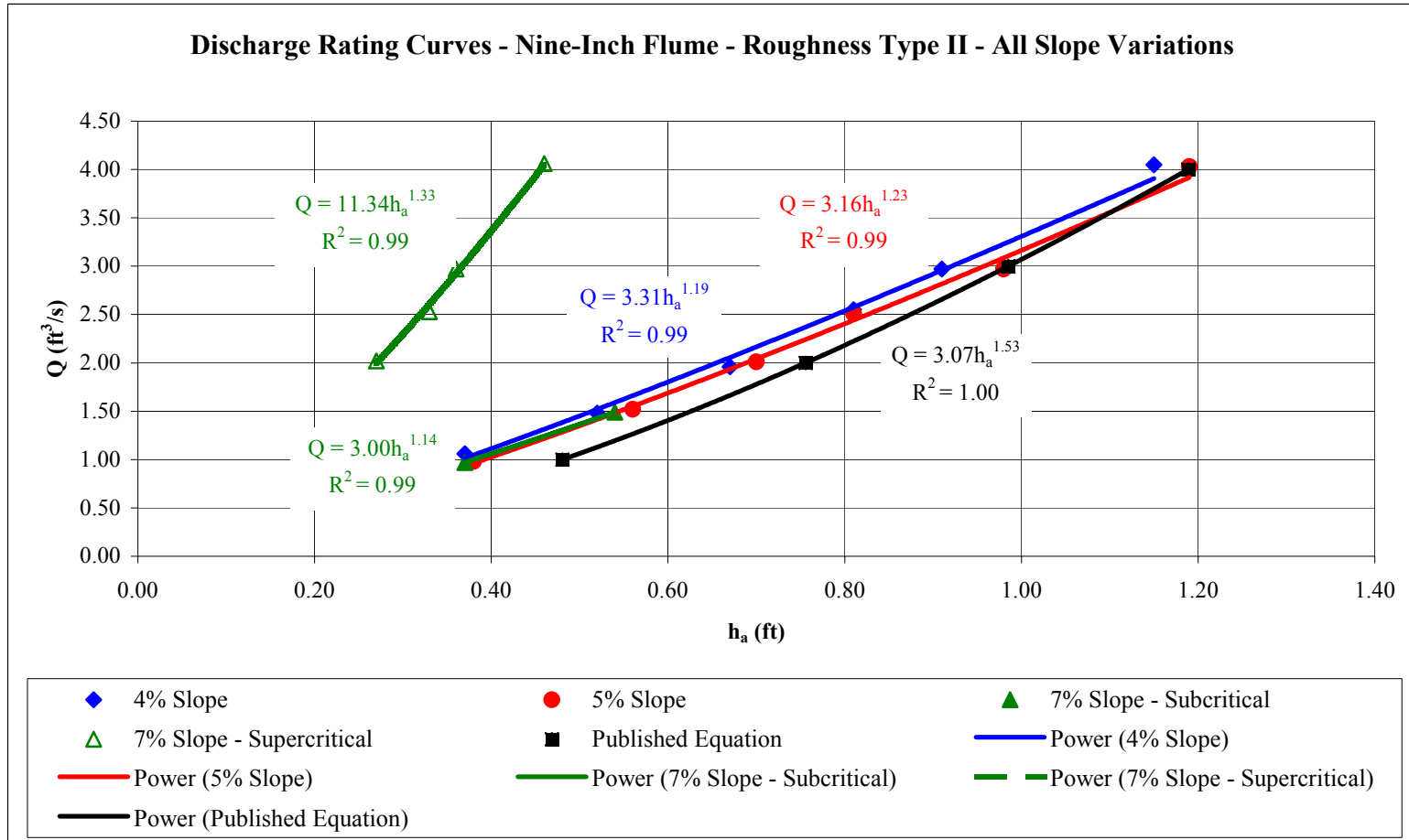


Figure 4.6: Discharge Rating Curves for the 9-inch Flume – Roughness Type II (All Slopes)

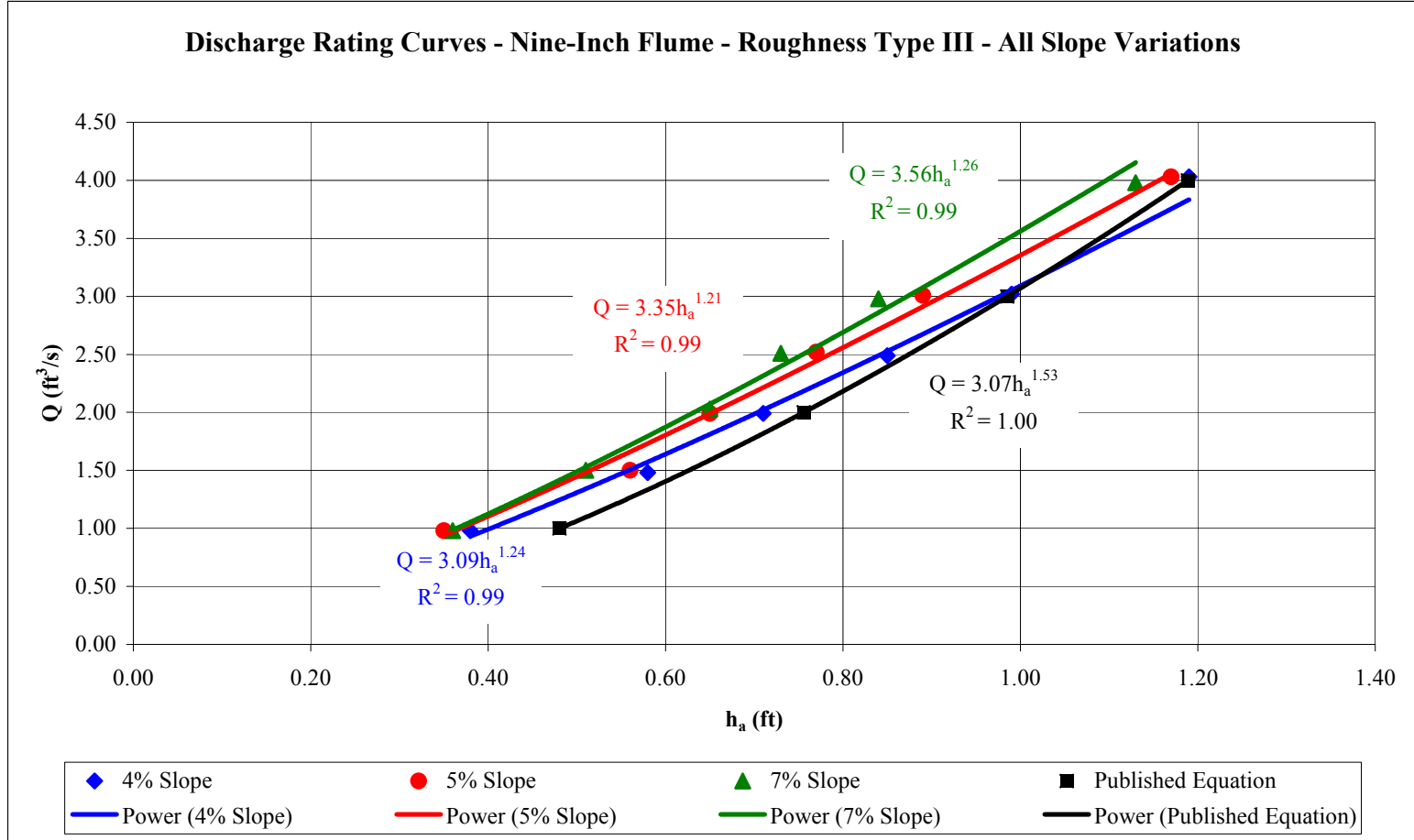


Figure 4.7: Discharge Rating Curves for the 9-inch Flume – Roughness Type III (All Slopes)

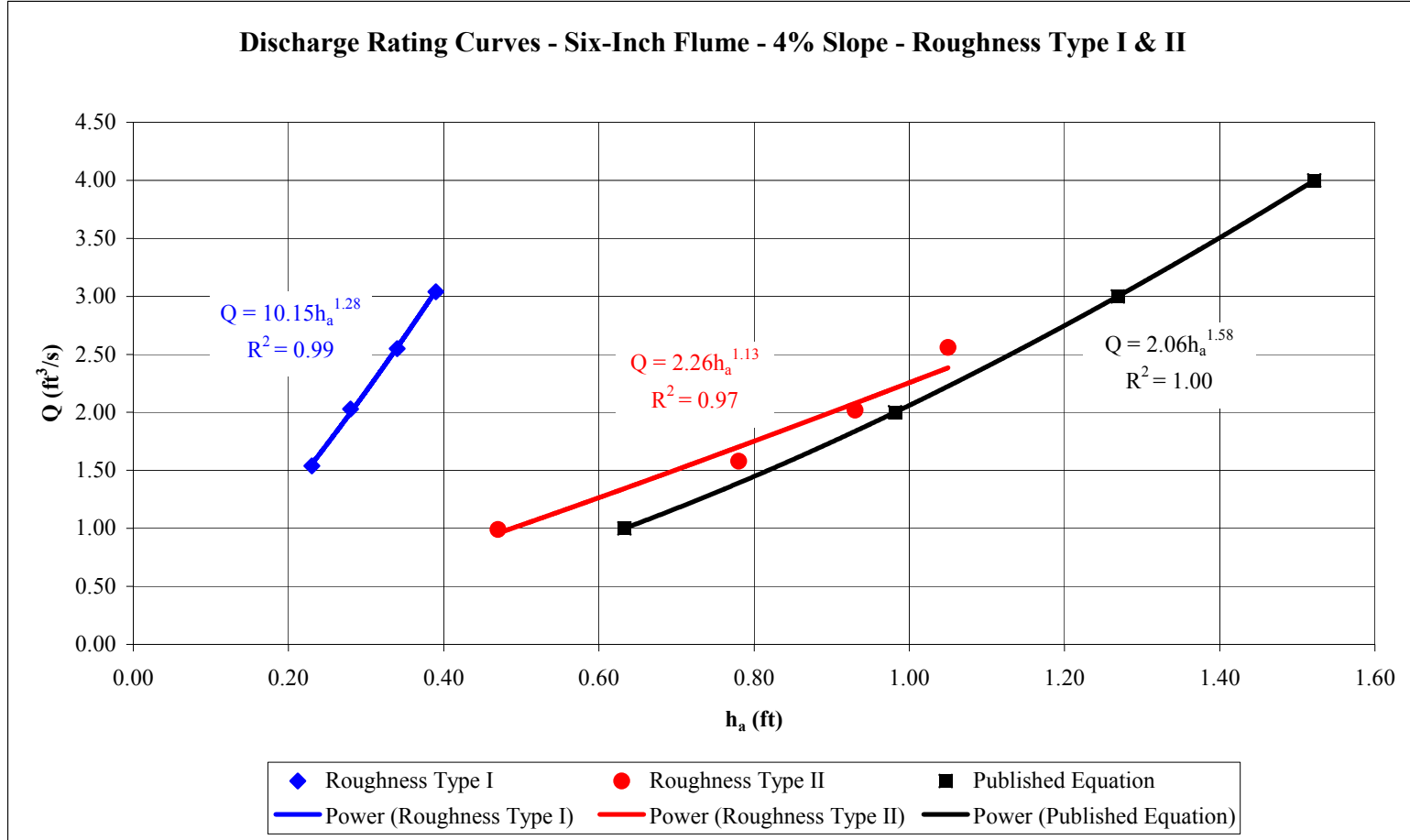


Figure 4.8: Discharge Rating Curves for the 6-inch Flume – 4% Slope (Roughness Types I and II)

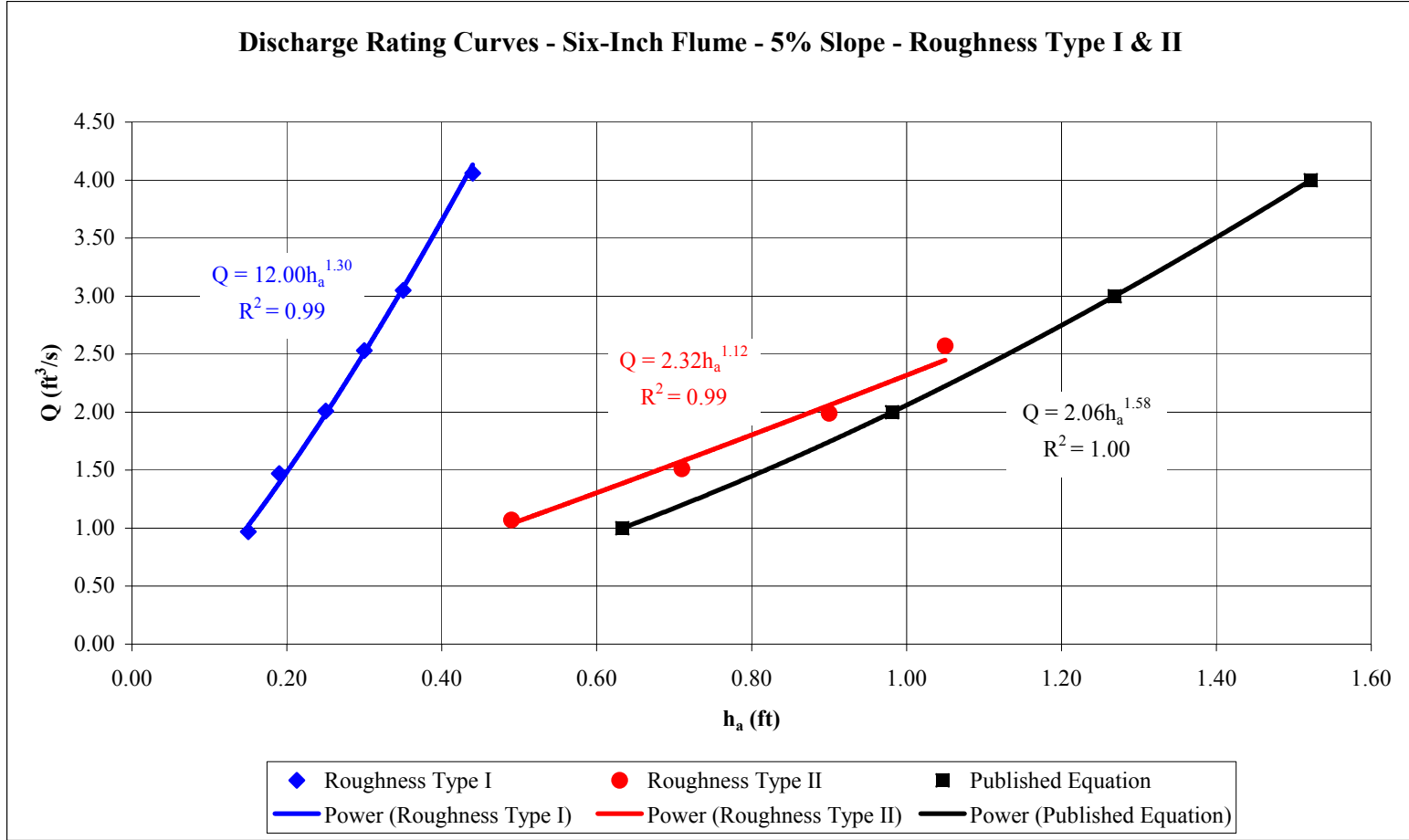


Figure 4.9: Discharge Rating Curves for the 6-inch Flume – 5% Slope (Roughness Types I and II)

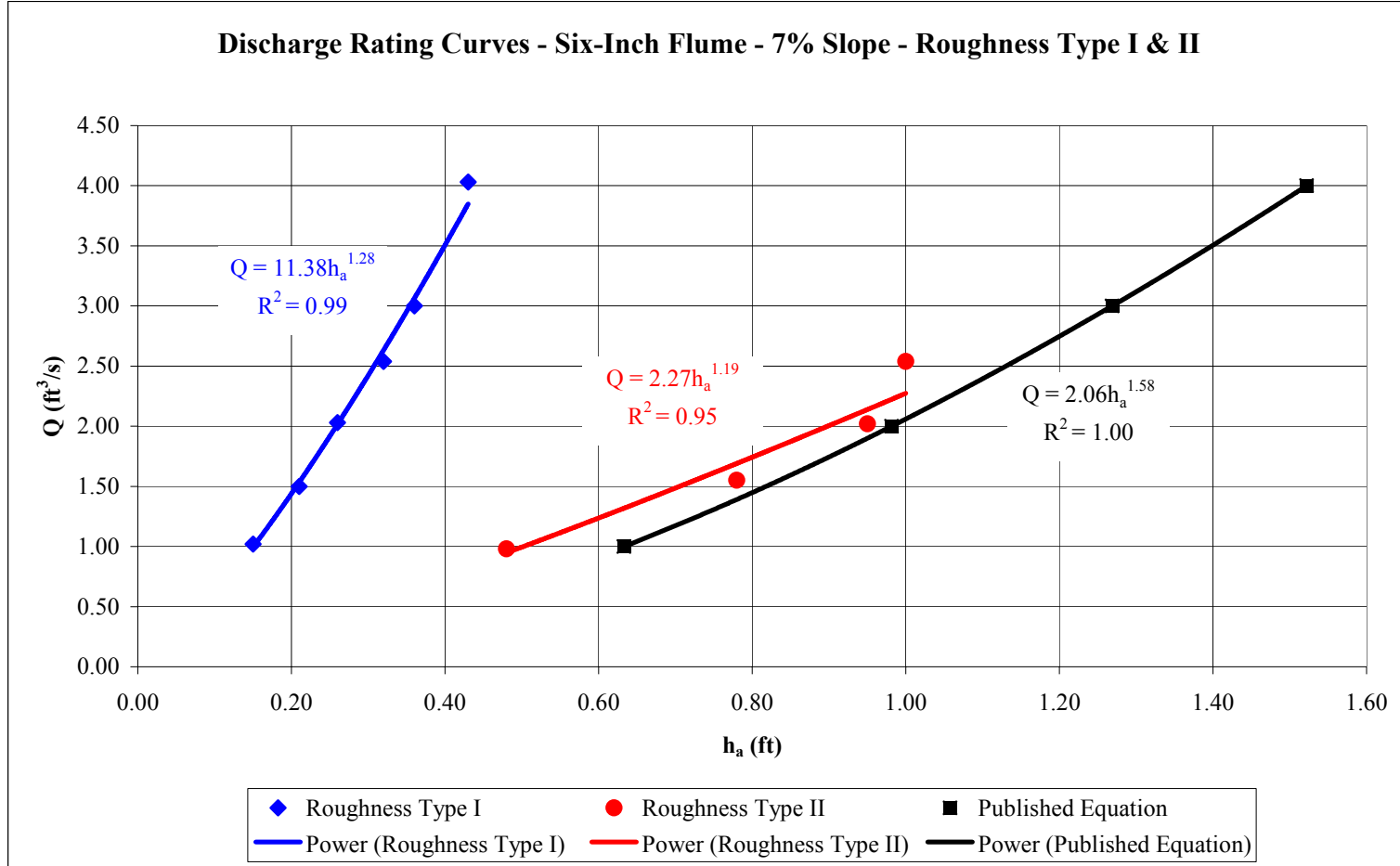


Figure 4.10: Discharge Rating Curves for the 6-inch Flume – 7% Slope (Roughness Types I and II)

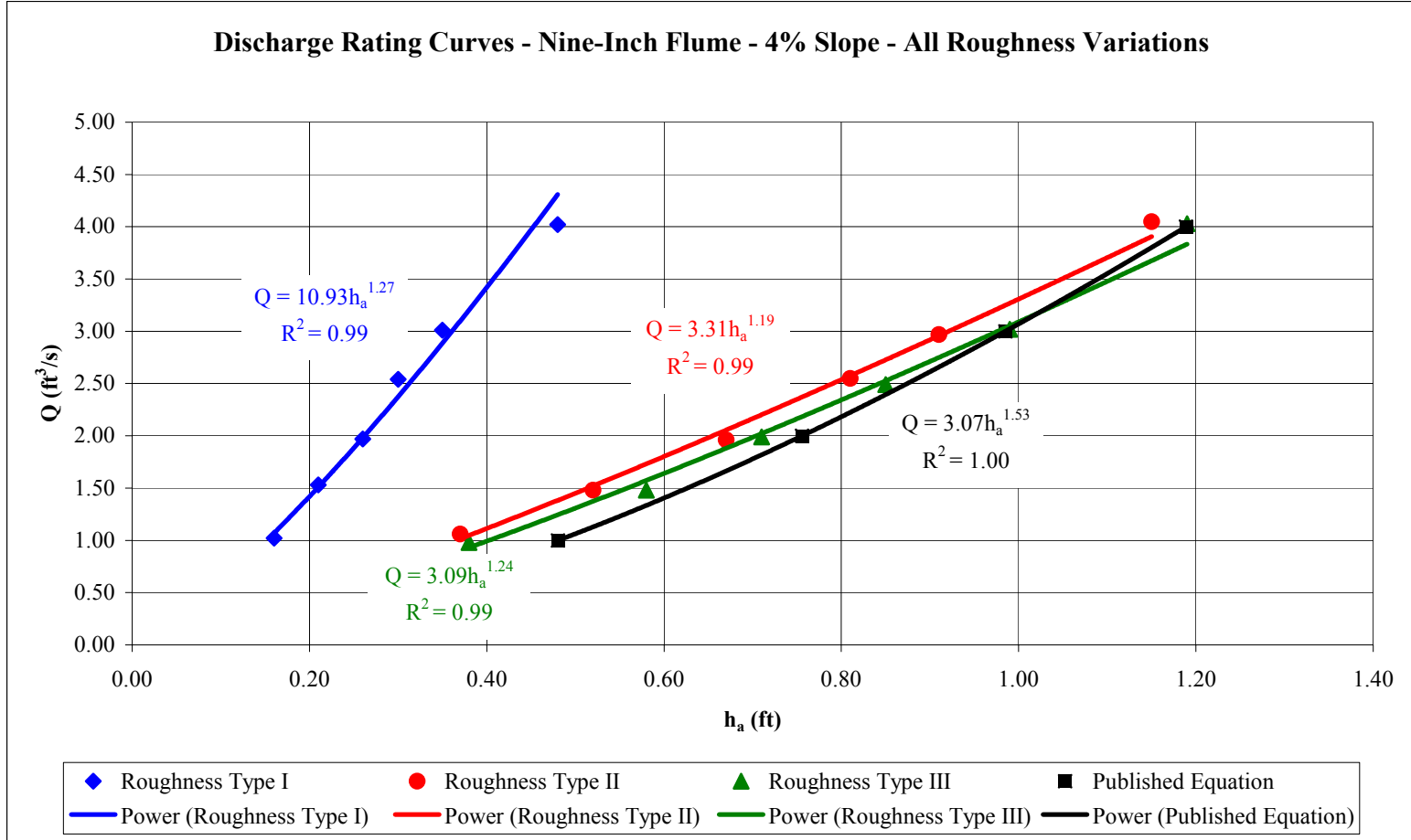


Figure 4.11: Discharge Rating Curves for the 9-inch Flume – 4% Slope (All Roughness Variations)

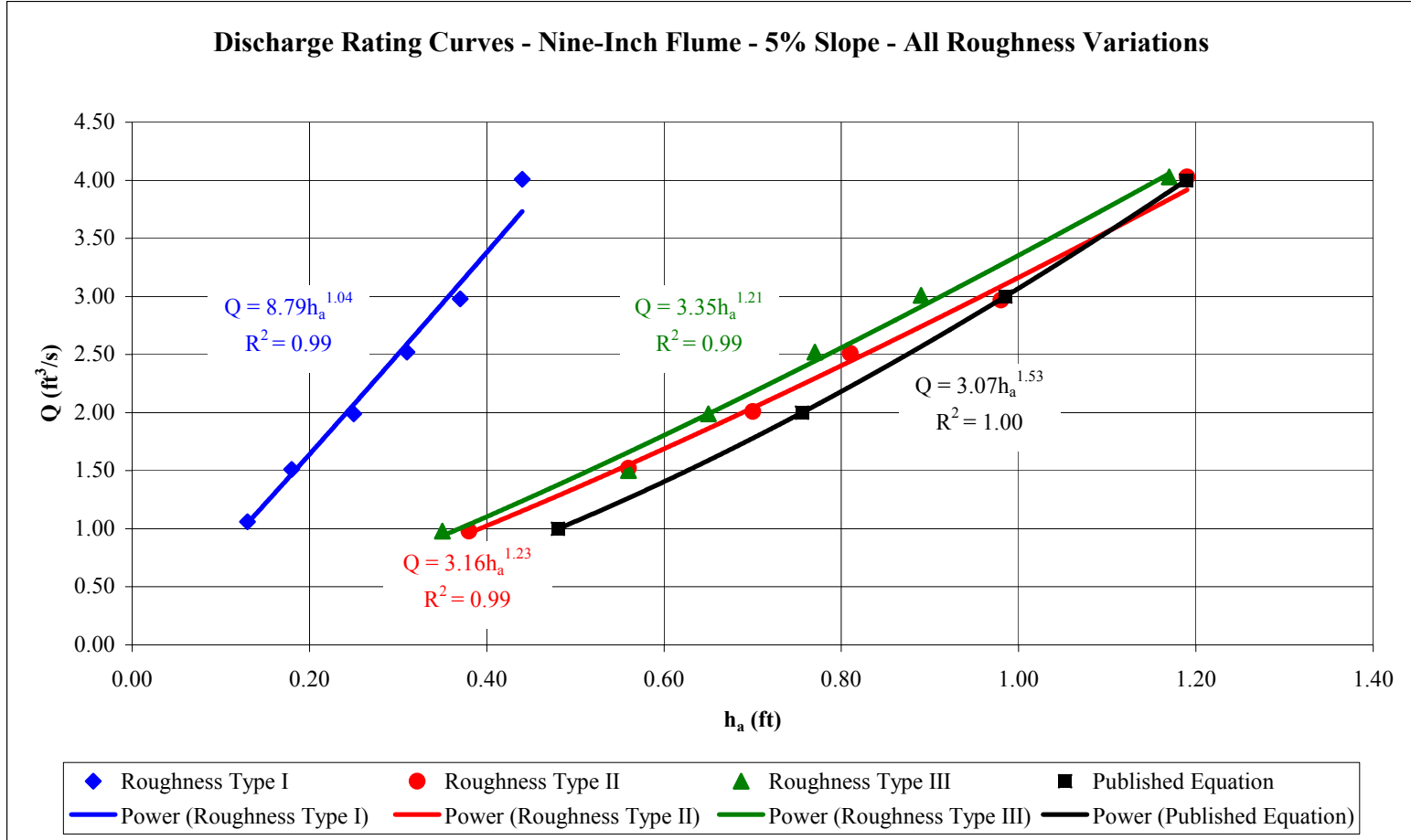


Figure 4.12: Discharge Rating Curves for the 9-inch Flume – 5% Slope (All Roughness Variations)

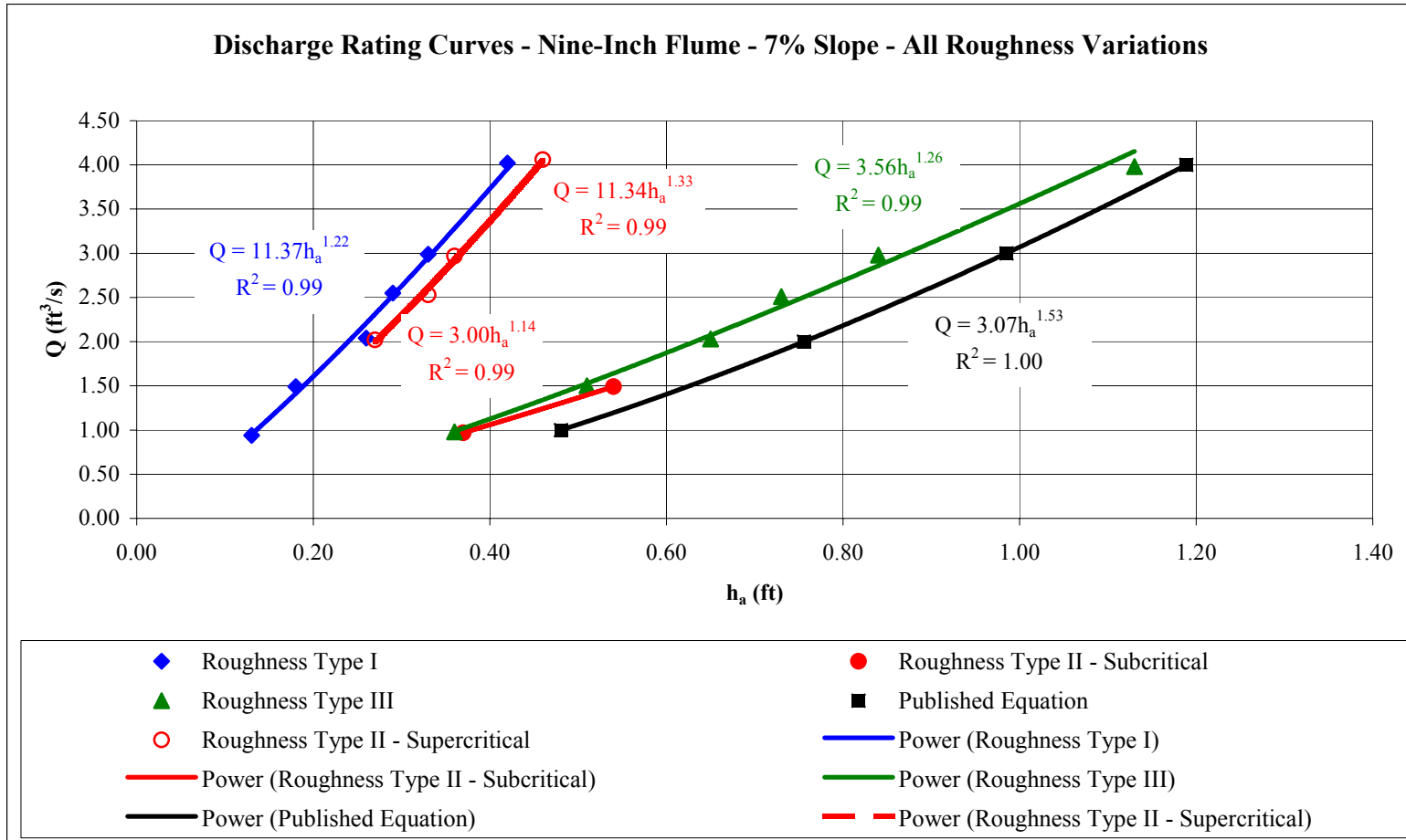


Figure 4.13: Discharge Rating Curves for the 9-inch Flume – 7% Slope (All Roughness Variations)

4.4 SENSITIVITY ANALYSIS

The empirical relationships presented in Table 4.5 were analyzed for sensitivity to variations in roughness and slope. Equations were first categorized into groups based upon flume size, slope, and roughness. Once grouped, the empirical equations shown in Table 4.5 were utilized to compute discharges for incremental values of h_a . All equations presented in Table 4.5 were developed under different conditions, yielding different equations that produce different discharge values for the same h_a value. Performing a statistical analysis on the different discharge values computed for the same h_a value would determine the sensitivity of the empirically developed equations to slope and roughness. Computing discharges for a range of h_a values further allows a sensitivity analysis of slope and roughness to be conducted over a range of discharges.

For comparison purposes, only the range of h_a applicable to all equations within a group was utilized for sensitivity analysis. The range of applicable h_a values for each group was determined from the range of h_a values recorded during testing. Discharges were then computed utilizing the developed equations and the applicable h_a range. Computed discharges were statistically compared by computing the mean discharge and standard deviation for each increment of h_a . Percent differences, computed as the standard deviation divided by the average discharge, were also computed for every value of h_a within each group. This allowed for a direct comparison between the different groupings of equations.

In order to determine the sensitivity to variations in slope, analysis was carried out within roughness types. Five (5) groupings of equations were utilized for the analysis as shown in Tables 4.6 through 4.10. Each grouping was produced by combining the empirical equations gathered for all three (3) slopes of a given roughness. Groupings were also broken down into

Parshall flume throat width, yielding two (2) independent groupings for the 6-inch flume testing and three (3) for the 9-inch flume testing. Plots of the data used for the development of the equations in Table 4.5 are presented as Figures 4.3 through 4.7. Data presented in Tables 4.6 through 4.10 provide the sensitivity analysis for the applicable range of h_a values determined for each grouping. Expanded versions of Tables 4.6, 4.9, and 4.10 that contain data not used for the sensitivity analysis are located in Appendix A.

Table 4.6: Six-inch Parshall Flume Roughness Type I – Variation in Slope

6-inch Parshall Flume Roughness Type I						
4% Slope		5% Slope		7% Slope		
Supercritical Regime		Supercritical Regime		Supercritical Regime		
$Q = 10.15h_a^{1.28}$		$Q = 12.00h_a^{1.30}$		$Q = 11.38h_a^{1.28}$		
h_a (ft)	Q (ft³/s)	Q (ft³/s)	Q (ft³/s)	Average Q (ft³/s)	Standard Deviation σ	Percent Difference
0.15	0.90	1.02	1.00	0.97	0.07	6.94
0.20	1.29	1.48	1.45	1.41	0.10	7.14
0.25	1.72	1.98	1.93	1.88	0.14	7.30
0.30	2.17	2.51	2.44	2.37	0.18	7.43
0.35	2.65	3.07	2.97	2.89	0.22	7.55
0.40	3.14	3.65	3.52	3.44	0.26	7.66
0.45	3.65	4.25	4.10	4.00	0.31	7.75

Table 4.7: Six-inch Parshall Flume Roughness Type II – Variation in Slope

6-inch Parshall Flume Roughness Type II						
4% Slope		5% Slope		7% Slope		
Subcritical Regime		Subcritical Regime		Subcritical Regime		Subcritical Regime
$Q = 2.26h_a^{1.13}$		$Q = 2.32h_a^{1.12}$		$Q = 2.27h_a^{1.19}$		Average
h_a (ft)	Q (ft ³ /s)	Q (ft ³ /s)	Q (ft ³ /s)	Q (ft ³ /s)	Standard Deviation σ	Percent Difference
0.50	1.03	1.07	0.99	1.03	0.04	3.51
0.55	1.15	1.19	1.11	1.15	0.04	3.18
0.60	1.27	1.31	1.24	1.27	0.04	2.88
0.65	1.39	1.43	1.36	1.39	0.04	2.62
0.70	1.51	1.56	1.48	1.52	0.04	2.37
0.75	1.63	1.68	1.61	1.64	0.04	2.16
0.80	1.76	1.81	1.74	1.77	0.03	1.96
0.85	1.88	1.93	1.87	1.90	0.03	1.79
0.90	2.01	2.06	2.00	2.02	0.03	1.64
0.95	2.13	2.19	2.14	2.15	0.03	1.51
1.00	2.26	2.32	2.27	2.28	0.03	1.41
1.05	2.39	2.45	2.41	2.41	0.03	1.33

Table 4.8: Nine-inch Parshall Flume Roughness Type I – Variation in Slope

9-inch Parshall Flume Roughness Type I						
4% Slope		5% Slope		7% Slope		
Supercritical Regime		Supercritical Regime		Supercritical Regime		Supercritical Regime
$Q = 10.93h_a^{1.27}$		$Q = 8.79h_a^{1.04}$		$Q = 11.37h_a^{1.22}$		Average
h_a (ft)	Q (ft ³ /s)	Q (ft ³ /s)	Q (ft ³ /s)	Q (ft ³ /s)	Standard Deviation σ	Percent Difference
0.15	0.98	1.22	1.12	1.11	0.12	10.87
0.20	1.42	1.65	1.60	1.55	0.12	7.86
0.25	1.88	2.08	2.10	2.02	0.12	5.96
0.30	2.37	2.51	2.62	2.50	0.12	4.99
0.35	2.88	2.95	3.16	3.00	0.14	4.82
0.40	3.41	3.39	3.72	3.51	0.18	5.21
0.45	3.96	3.83	4.29	4.03	0.24	5.89

Table 4.9: Nine-inch Parshall Flume Roughness Type II – Variation in Slope

9-inch Parshall Flume Roughness Type II						
4% Slope		5% Slope		7% Slope		
Subcritical Regime		Subcritical Regime		Subcritical Regime		Subcritical Regime
$Q = 3.31h_a^{1.19}$		$Q = 3.16h_a^{1.23}$		$Q = 3.00h_a^{1.14}$		Average
h_a (ft)	Q (ft ³ /s)	Q (ft ³ /s)	Q (ft ³ /s)	Q (ft ³ /s)	Standard Deviation σ	Percent Difference
0.40	1.11	1.02	1.06	1.06	0.04	4.22
0.45	1.28	1.18	1.21	1.22	0.05	4.10
0.50	1.45	1.35	1.36	1.39	0.06	4.05
0.55	1.63	1.51	1.52	1.55	0.06	4.05

Table 4.10: Nine-inch Parshall Flume Roughness Type III – Variation in Slope

9-inch Parshall Flume Roughness Type III						
4% Slope		5% Slope		7% Slope		
Subcritical Regime		Subcritical Regime		Subcritical Regime		Subcritical Regime
$Q = 3.09h_a^{1.24}$		$Q = 3.35h_a^{1.21}$		$Q = 3.56h_a^{1.26}$		Average
h_a (ft)	Q (ft ³ /s)	Q (ft ³ /s)	Q (ft ³ /s)	Q (ft ³ /s)	Standard Deviation σ	Percent Difference
0.40	0.99	1.11	1.12	1.07	0.07	6.60
0.45	1.15	1.27	1.30	1.24	0.08	6.61
0.50	1.31	1.45	1.49	1.41	0.09	6.63
0.55	1.47	1.63	1.68	1.59	0.11	6.66
0.60	1.64	1.81	1.87	1.77	0.12	6.70
0.65	1.81	1.99	2.07	1.96	0.13	6.74
0.70	1.99	2.18	2.27	2.14	0.15	6.78
0.75	2.16	2.37	2.48	2.34	0.16	6.83
0.80	2.34	2.56	2.69	2.53	0.17	6.87
0.85	2.53	2.75	2.90	2.73	0.19	6.92
0.90	2.71	2.95	3.12	2.93	0.20	6.97
0.95	2.90	3.15	3.34	3.13	0.22	7.02
1.00	3.09	3.35	3.56	3.33	0.24	7.06
1.05	3.28	3.55	3.79	3.54	0.25	7.11
1.10	3.48	3.76	4.01	3.75	0.27	7.16
1.15	3.67	3.97	4.25	3.96	0.29	7.20

In order to determine the sensitivity of variations in roughness, analysis was carried out within slopes. Six (6) groupings of equations were utilized for the analysis. The groupings for the 9-inch flume are shown in Tables 4.11 through 4.13. Each grouping was produced by combining the empirical equations gathered for all three (3) roughness variations for a given slope. Groupings were also broken down into flume width, yielding three (3) independent groupings for the 6-inch flume testing and three (3) for the 9-inch flume testing. Plots of the data used for the equation development of Configurations 7 through 15 in Table 4.5 are presented as Figures 4.8 through 4.13. Data presented in Tables 4.11 through 4.14 provide the sensitivity analysis for the applicable range of h_a values determined for each grouping from the 9-inch flume. Since testing of the 6-inch flume only included roughness Types I and II that produced only one supercritical and one subcritical flow condition, no applicable range of h_a values could be determined and an analysis of roughness sensitivity was not possible. Tables that present 6-inch testing data and expanded versions of Tables 4.11 through 4.14 are located in Appendix A.

Table 4.11: Nine-inch Parshall Flume 4% Slope – Variation in Roughness

9-inch Parshall Flume 4% Slope									
	Roughness Type I	Roughness Type II	Roughness Type III						
	Supercritical Regime	Subcritical Regime	Subcritical Regime	Subcritical Regime	Subcritical Regime	Subcritical Regime	Combined Regime	Combined Regime	Combined Regime
	$Q = 10.93h_a^{1.27}$	$Q = 3.31h_a^{1.19}$	$Q = 3.09h_a^{1.24}$	Average	Standard	Percent	Average	Standard	Percent
h_a (ft)	Q (ft ³ /s)	Deviation σ	Difference	Q (ft ³ /s)	Deviation σ	Difference			
0.40	3.41	1.11	0.99	1.05	0.09	8.09	1.84	1.36	74.20
0.45	3.96	1.28	1.15	1.21	0.09	7.68	2.13	1.59	74.60
0.50	N/A	1.45	1.31	1.38	0.10	7.31	N/A	N/A	N/A
0.55	N/A	1.63	1.47	1.55	0.11	6.97	N/A	N/A	N/A
0.60	N/A	1.80	1.64	1.72	0.11	6.66	N/A	N/A	N/A
0.65	N/A	1.98	1.81	1.90	0.12	6.38	N/A	N/A	N/A
0.70	N/A	2.17	1.99	2.08	0.13	6.12	N/A	N/A	N/A
0.75	N/A	2.35	2.16	2.26	0.13	5.88	N/A	N/A	N/A
0.80	N/A	2.54	2.34	2.44	0.14	5.65	N/A	N/A	N/A
0.85	N/A	2.73	2.53	2.63	0.14	5.44	N/A	N/A	N/A
0.90	N/A	2.92	2.71	2.82	0.15	5.23	N/A	N/A	N/A
0.95	N/A	3.11	2.90	3.01	0.15	5.04	N/A	N/A	N/A
1.00	N/A	3.31	3.09	3.20	0.16	4.86	N/A	N/A	N/A
1.05	N/A	3.51	3.28	3.40	0.16	4.69	N/A	N/A	N/A
1.10	N/A	3.71	3.48	3.59	0.16	4.52	N/A	N/A	N/A
1.15	N/A	3.91	3.67	3.79	0.17	4.37	N/A	N/A	N/A
1.20	N/A	4.11	3.87	3.99	0.17	4.22	N/A	N/A	N/A

N/A = not applicable

Table 4.12: Nine-inch Parshall Flume 5% Slope – Variation in Roughness

9-inch Parshall Flume 5% Slope									
	Roughness Type I	Roughness Type II	Roughness Type III						
	Supercritical Regime	Subcritical Regime	Subcritical Regime	Subcritical Regime	Subcritical Regime	Subcritical Regime	Combined Regime	Combined Regime	Combined Regime
	$Q = 8.79h_a^{1.04}$	$Q = 3.16h_a^{1.23}$	$Q = 3.35h_a^{1.21}$	Average	Standard Deviation	Percent Difference	Average	Standard Deviation	Percent Difference
h_a (ft)	Q (ft³/s)	Q (ft³/s)	Q (ft³/s)	Q (ft³/s)	σ		Q (ft³/s)	σ	
0.40	3.39	1.02	1.11	1.06	0.06	5.42	1.84	1.34	73.00
0.45	3.83	1.18	1.27	1.23	0.06	5.26	2.10	1.50	71.69
0.50	N/A	1.35	1.45	1.40	0.07	5.11	N/A	N/A	N/A
0.55	N/A	1.51	1.63	1.57	0.08	4.97	N/A	N/A	N/A
0.60	N/A	1.69	1.81	1.75	0.08	4.85	N/A	N/A	N/A
0.65	N/A	1.86	1.99	1.92	0.09	4.74	N/A	N/A	N/A
0.70	N/A	2.04	2.18	2.11	0.10	4.63	N/A	N/A	N/A
0.75	N/A	2.22	2.37	2.29	0.10	4.53	N/A	N/A	N/A
0.80	N/A	2.40	2.56	2.48	0.11	4.44	N/A	N/A	N/A
0.85	N/A	2.59	2.75	2.67	0.12	4.36	N/A	N/A	N/A
0.90	N/A	2.78	2.95	2.86	0.12	4.28	N/A	N/A	N/A
0.95	N/A	2.97	3.15	3.06	0.13	4.20	N/A	N/A	N/A
1.00	N/A	3.16	3.35	3.26	0.13	4.13	N/A	N/A	N/A
1.05	N/A	3.36	3.55	3.45	0.14	4.06	N/A	N/A	N/A
1.10	N/A	3.55	3.76	3.66	0.15	3.99	N/A	N/A	N/A
1.15	N/A	3.75	3.97	3.86	0.15	3.93	N/A	N/A	N/A
1.20	N/A	3.95	4.18	4.07	0.16	3.87	N/A	N/A	N/A

N/A = not applicable

Table 4.13: Nine-inch Parshall Flume 7% Slope – Variation in Roughness

9-inch Parshall Flume 7% Slope													
	Roughness Type I	Roughness Type II	Roughness Type II	Roughness Type III									
	Super-critical Regime	Super-critical Regime	Sub-critical Regime	Sub-critical Regime	Super-critical Regime	Super-critical Regime	Super-critical Regime	Sub-critical Regime	Sub-critical Regime	Sub-critical Regime	Com-bined Regime	Com-bined Regime	Com-bined Regime
	$Q = 11.37h_a^{1.22}$	$Q = 11.34h_a^{1.33}$	$Q = 3.00h_a^{1.14}$	$Q = 3.56h_a^{1.26}$	Average	Standard	Percent	Average	Standard	Percent	Average	Standard	Percent
h_a (ft)	Q (ft ³ /s)	Deviation σ	Difference	Q (ft ³ /s)	Deviation σ	Difference	Q (ft ³ /s)	Deviation σ	Difference				
0.25	2.10	1.79	N/A	N/A	1.94	0.21	10.95	N/A	N/A	N/A	N/A	N/A	N/A
0.30	2.62	2.29	N/A	N/A	2.45	0.23	9.54	N/A	N/A	N/A	N/A	N/A	N/A
0.35	3.16	2.81	N/A	N/A	2.98	0.25	8.34	N/A	N/A	N/A	N/A	N/A	N/A
0.40	3.72	3.35	1.06	1.12	3.54	0.26	7.31	1.09	0.05	4.33	2.31	1.42	61.44
0.45	4.29	3.92	1.21	1.30	4.11	0.26	6.39	1.25	0.07	5.32	2.68	1.65	61.71
0.50	N/A	N/A	1.36	1.49	N/A	N/A	N/A	1.42	0.09	6.22	N/A	N/A	N/A
0.55	N/A	N/A	1.52	1.68	N/A	N/A	N/A	1.60	0.11	7.02	N/A	N/A	N/A

N/A = not applicable

4.5 DISCUSSION OF RESULTS

At the completion of testing, the database presented in Table 4.3 was compiled. Variables governing the physical processes of the experiment, included within the database, were determined by the study team. From the database, sixteen (16) empirical calibration equations were developed from the fifteen (15) testing configurations as presented in Table 4.5. Two calibration equations were developed for Configuration 12, given that both subcritical and supercritical regimes were present during testing. A sensitivity analysis was then conducted on the sixteen (16) calibration equations to determine the sensitivity of the developed equations to variations in upstream roughness and bed slope. The results of this analysis are presented in the following sections.

4.5.1 SLOPE SENSITIVITY ANALYSIS

As shown in Tables 4.6 through 4.10 an analysis of slope sensitivity was conducted on the sixteen (16) equations presented in Table 4.5. In order to determine the sensitivity of these equations to upstream bed slope, equations were grouped into categories based on flume width and constant roughness for analysis. The results of analysis from the 6- and 9-inch flumes are presented below.

Six-inch Analysis Results:

- Roughness Type I
 - All variations in slope produced supercritical flow;
 - The applicable range of h_a values was determined to be 0.15 to 0.45 feet;
 - The highest percent difference from the average discharge was 7.75%, as presented in Table 4.6;

- The lowest percent difference from the average discharge was 6.94%, as presented in Table 4.6; and
- The equations, shown in Figure 4.3, all had a goodness of fit (R^2) value greater than 0.99, indicating that 99 percent of the variability in the data was explained by the empirical equations.
- Roughness Type II
 - All variations in slope produced subcritical flow;
 - The applicable range of h_a values was determined to be 0.50 to 1.05 feet;
 - The highest percent difference from the average discharge was 3.51%, as presented in Table 4.7;
 - The lowest percent difference from the average discharge was 1.33%, as presented in Table 4.7;
 - The equations, shown in Figure 4.4, all had a goodness of fit (R^2) value greater than 0.95, indicating that 95 percent of the variability in the data was explained by the empirical equations; and
 - The empirical equations, as shown in Figure 4.4, all tend to approach the published rating equation as discharge increases, indicating that the local turbulence at the entrance of the flume is decreasing. This implies that the flow is approaching flow conditions similar to those for the development of the published rating equation.

9-inch Analysis Results:

- Roughness Type I
 - All variations in slope produced supercritical flow;

- The applicable range of h_a values was determined to be 0.15 to 0.45 feet;
 - The highest percent difference from the average discharge was 10.87%, as presented in Table 4.8;
 - The lowest percent difference from the average discharge was 4.82%, as presented in Table 4.8; and
 - The equations, shown in Figure 4.5, all had a goodness of fit (R^2) value greater than 0.99, indicating that 99 percent of the variability in the data was explained by the empirical equations.
- Roughness Type II
 - The 4% and 5% slopes produced subcritical flow and the 7% slope produced both subcritical and supercritical flows;
 - For the subcritical equations only, the applicable range of h_a values was determined to be 0.40 to 0.55 feet;
 - For the subcritical equations only, the highest percent difference from the average discharge was 4.22%, as presented in Table 4.9;
 - For the subcritical equations only, the lowest percent difference from the average discharge was 4.05%, as presented in Table 4.9;
 - As there was only one supercritical equation, no comparisons were performed;
 - The equations, shown in Figure 4.6, all had a goodness of fit (R^2) value greater than 0.99, indicating that 99 percent of the variability in the data was explained by the empirical equations; and
 - The subcritical empirical equations, as shown in Figure 4.6, all tend to approach the published rating equation as discharge increases, indicating that the local

turbulence at the entrance of the flume is decreasing. This implies that the flow is approaching flow conditions similar to those for the development of the published rating equation.

- Roughness Type III
 - All variations in slope produced subcritical flow;
 - The applicable range of h_a values was determined to be 0.40 to 1.15 feet;
 - The highest percent difference from the average discharge was 7.20%, as presented in Table 4.10;
 - The lowest percent difference from the average discharge was 6.60%, as presented in Table 4.10; and
 - The equations, shown in Figure 4.7, all had a goodness of fit (R^2) value greater than 0.99, indicating that 99 percent of the variability in the data was explained by the empirical equations; and
 - The empirical equations, as shown in Figure 4.7, all tend to approach the published rating equation as discharge increases, indicating that the local turbulence at the entrance of the flume is decreasing. This implies that the flow is approaching flow conditions similar to those for the development of the published rating equation.

The results of this analysis show values of standard deviations less than 0.31 cfs from the average discharge. With the exception of one (1) test, all percent differences were less than 9%. In general, the subcritical empirical equations developed and examined for slope sensitivity tend to approach the published rating equation as discharge increases, indicating that the local turbulence at the entrance of the flume is decreasing. This implies that the flow is approaching

flow conditions similar to those for the development of the published rating equation. All of the equations presented in Figures 4.3 through 4.7 have a measure of goodness of fit (R^2) greater than 0.95, indicating that at least 95 percent of the variability in the data can be explained with the equations.

4.5.2 ROUGHNESS SENSITIVITY ANALYSIS

As shown in Tables 4.11 through 4.16 an analysis of roughness sensitivity was conducted on the sixteen (16) equations presented in Table 4.5. In order to determine the sensitivity of these equations to upstream roughness, equations were grouped into categories based on flume width and slope for analysis. The results of analysis from the 9-inch flume for a given slope are presented below. Since testing of the 6-inch flume only included roughness Types I and II that produced only one supercritical and one subcritical flow condition, an analysis of roughness sensitivity was not possible.

9-inch Analysis Results:

- 4% Slope
 - Roughness Type I produced a supercritical flow condition and roughness Types II and III produced subcritical flow;
 - For the subcritical equations only, the applicable range of h_a values was determined to be 0.40 to 1.20 feet;
 - For the subcritical equations only, the highest percent difference from the average discharge was 8.09%, as presented in Table 4.14;
 - For the subcritical equations only, the lowest percent difference from the average discharge was 4.22%, as presented in Table 4.14;

- As there was only one supercritical equation, an analysis of roughness sensitivity in the supercritical regime was not performed;
 - The equations, shown in Figure 4.11, all had a goodness of fit (R^2) value greater than 0.99, indicating that 99 percent of the variability in the data was explained by the empirical equations; and
 - The subcritical empirical equations, as shown in Figure 4.11, all tend to approach the published rating equation as discharge increases, indicating that the local turbulence at the entrance of the flume is decreasing. This implies that the flow is approaching flow conditions similar to those for the development of the published rating equation.
- 5% Slope
 - Roughness Type I produced a supercritical flow condition and roughness Types II and III produced subcritical flow;
 - For the subcritical equations only, the applicable range of h_a values was determined to be 0.40 to 1.20 feet;
 - For the subcritical equations only, the highest percent difference from the average discharge was 5.42%, as presented in Table 4.15;
 - For the subcritical equations only, the lowest percent difference from the average discharge was 3.87%, as presented in Table 4.15;
 - As there was only one supercritical equation, an analysis of roughness sensitivity in the supercritical regime was not performed;

- The equations, shown in Figure 4.12, all had a goodness of fit (R^2) value greater than 0.99, indicating that 99 percent of the variability in the data was explained by the empirical equations; and
- The subcritical empirical equations, as shown in Figure 4.12, all tend to approach the published rating equation as discharge increases, indicating that the local turbulence at the entrance of the flume is decreasing. This implies that the flow is approaching flow conditions similar to those for the development of the published rating equation.
- 7% Slope Constant
 - Roughness Type I produced a supercritical flow condition, roughness Type II produced both supercritical and subcritical flows, and roughness Type III produced subcritical flow;
 - For the subcritical equations only, the applicable range of h_a values was determined to be 0.40 to 0.55 feet;
 - For the subcritical equations only, the highest percent difference from the average discharge was 7.02%, as presented in Table 4.16;
 - For the subcritical equations only, the lowest percent difference from the average discharge was 4.33%, as presented in Table 4.16;
 - For the supercritical equations only, the applicable range of h_a values was determined to be 0.25 to 0.45 feet;
 - For the supercritical equations only, the highest percent difference from the average discharge was 10.95%, as presented in Table 4.16;

- For the supercritical equations only, the lowest percent difference from the average discharge was 6.39%, as presented in Table 4.16
- The equations, shown in Figure 4.13, all had a goodness of fit (R^2) value greater than 0.99, indicating that 99 percent of the variability in the data was explained by the empirical equations; and
- The subcritical empirical equations, as shown in Figure 4.13, all tend to approach the published rating equation as discharge increases, indicating that the local turbulence at the entrance of the flume is decreasing. This implies that the flow is approaching flow conditions similar to those for the development of the published rating equation.

The results of this analysis show values of standard deviations less than 0.17 cfs from the average discharge and percent differences less than approximately 8% for the subcritical equations only. In general, the subcritical empirical equations developed and examined for roughness sensitivity all tend to approach the published rating equation as discharge increases, indicating that the local turbulence at the entrance of the flume is decreasing. This implies that the flow is approaching flow conditions similar to those for the development of the published rating equation. There were not enough conditions in which supercritical flow occurred across varying roughness to warrant any conclusive remarks. All of the equations presented in Figures 4.8 through 4.13 have a measure of goodness of fit (R^2) greater than 0.95, indicating that at least 95 percent of the variability in the data can be explained with the equations.

4.5.3 FLOW REGIME OBSERVATIONS

During the course of testing, supercritical and subcritical flow regimes were observed. In general, roughness Type I, in conjunction with both the 6- and 9-inch flumes produced

supercritical flow conditions upstream of the flume entrance. Roughness Type II, in conjunction with the 6-inch flume, produced subcritical flow while roughness Type II, in conjunction with the 9-inch flumes, produced both supercritical and subcritical flows. Roughness Type III, in conjunction with the 6- and 9-inch flumes, produced subcritical flow. The difference in discharge measurements between the two flow regimes was found to be significant. For example, from Table 4.11 (9-inch flume with 4% slope), the reported percent difference from the average discharge of the two flow regimes was approximately 74%. Similarly, from Table 4.13 (9-inch flume with 7% slope), the reported percent difference from the average discharge of the two flow regimes was approximately 61%. Results from the 6-inch flume testing resulted in such a large deviation between discharges and h_a that a comparison could not be made, indicating the importance of flow regime upon the developed empirical equations. This importance is further demonstrated after examining the “a” column in Table 4.5. The developed empirical equations for the supercritical flow regime have “a” values ranging from 8.79 to 12.00, whereas the developed empirical equations for the subcritical flow regime have “a” values ranging from 2.26 to 3.56. The large difference of “a” values between the developed empirical equations for subcritical and supercritical confirms the significant sensitivity of an empirical calibration equation to flow regime.

5 CONCLUSIONS AND RECOMMENDATIONS

5.1 CONCLUSIONS

Parshall flume testing was conducted in the Hydraulics Laboratory at the ERC of CSU to determine the feasibility of calibrating a Parshall flume to accurately predict discharge in a supercritical flow regime. Testing was conducted in a 2-foot wide, 60-foot long re-circulating flume. Six-inch and 9-inch Parshall flumes were tested in conjunction with three (3) different slopes (4%, 5%, and 7%) with varying upstream roughness. Testing yielded a database of fifteen (15) total configurations and eighty-two (82) independent tests. 6-inch Parshall flume testing was comprised of six (6) configurations and twenty-eight (28) independent tests, while the 9-inch flume included nine (9) configurations and fifty-four (54) independent tests. Upon completion of testing, all recorded data were transferred to a database for analysis as presented in Table 4.3.

In order to address the first objective of Phase 2 of this study, the measured variables presented in the Table 4.3 were utilized to develop sixteen (16) equations of the general form of Parshall's equation. These sixteen (16) developed equations are presented in Table 4.5. All of the equations presented have a measure of goodness of fit (R^2) greater than 0.95, indicating that at least 95 percent of the variability in the data can be explained with the equations. Of the equations presented in Table 4.5, seven (7) of the sixteen (16) equations were developed for supercritical flow. With such high R^2 values, it was determined that it would be feasible to generate a calibration equation for Parshall flumes installed in supercritical flow regimes.

To meet the second objective of Phase 2 of this study, a slope sensitivity analysis was performed. The results of this analysis show values of standard deviations less than approximately 0.31 cfs from the average discharge with corresponding percent differences less

than approximately 11%. In general, the subcritical empirical equations developed and examined for slope sensitivity all tend to approach the published rating equation as discharge increases, indicating that the local turbulence at the entrance of the flume is decreasing.

To meet the third objective of Phase 2 of this study, a roughness sensitivity analysis was performed. In general, the subcritical empirical equations developed and examined for roughness sensitivity all tend to approach the published rating equation as discharge increases, indicating that the local turbulence at the entrance of the flume is decreasing. In the case of roughness variation, subcritical flow conditions show values of standard deviations less than approximately 0.17 cfs from the average discharge with corresponding percent differences less than approximately 8%. There were not sufficient conditions in which supercritical flow occurred for varying roughness to warrant any conclusive remarks.

In addition to satisfying the study objectives, some observations of flow regime were noted during testing. In general, roughness Type I, in conjunction with both the 6- and 9-inch flumes produced supercritical flow conditions upstream of the flume entrance. Roughness Type II, in conjunction with the 6-inch flume, produced subcritical flow while roughness Type II in conjunction with the 9-inch flume, produced both supercritical and subcritical flows. Roughness Type III, in conjunction with the 6- and 9-inch flumes, produced subcritical flow.

The difference in discharge measurements between the two flow regimes was found to be significant. For example, from Table 4.11 (9-inch flume with 4% slope), the reported percent difference from the average discharge of the two flow regimes was approximately 74%. Similarly, from Table 4.13 (9-inch flume with 7% slope), the reported percent difference from the average discharge of the two flow regimes was approximately 61%. Results from the 6-inch flume testing resulted in such a large deviation between discharges and h_a that a comparison

could not be made, indicating the importance of flow regime on the developed empirical equations. In the condition where a given Parshall flume experiences both supercritical and subcritical approach flow conditions, it is essential to know which portion of flows are subcritical and which portions are supercritical.

5.2 RECOMMENDATIONS

Results of this study indicate that calibration equations can be developed for Parshall flumes installed in supercritical flow conditions. Therefore, it is recommended that full-scale Parshall flume testing be performed. A proposal will be submitted to the NPS with a detailed scope of work pertaining to Phase 3.

6 REFERENCES

- Abt, S.R., Wittler, R.J., Ruff, J.D., LaGrone, D.L., Khattak, M.S., Nelson, J.F., Hinkle, N.E., and Lee, D.W. (1988). Development of Riprap Design Criteria by Riprap Testing in Flumes: Phase I. NUREG/CR-4651, U.S. Nuclear Regulatory Commission, Vol. 1.
- Bennett, R. S. (1972). Cutthroat Flume Discharge Relations. M.S. Thesis, Colorado State University, Department of Civil Engineering, Fort Collins, CO.
- Bos, M.G. *et al.* (1975, Revised 1989). Discharge Measurement Structures. International Institute for Land Reclamation and Improvement, The Netherlands.
- Chamberlin, A.R. (1957). Preliminary Model Tests of a Flume for Measuring Discharge of Steep Ephemeral Streams. Colorado Agricultural and Mechanical College, Rocky Mountain Forest and Range Experimental Station, Report CER57AC12, 28 p.
- Chery, D. L. Jr. and Smith, R.E. (1982). Field Rating Evaluation of a Large Supercritical Measurement Flume. *ISA Transactions*, 21(1):55-59.
- Chow, V. T. (1959). Open-channel Hydraulics. New York, NY: McGraw-Hill, 680 p.
- Julien, P.Y. (1998). Erosion and Sedimentation. Cambridge University Press, 280 p.
- Keller, R. J. (1984). Cutthroat Flume Characteristics. *J. Hydraulic Engineering*, 110(9):1248-1263.
- Kilpatrick, F.A. and Schneider, V.R. (1983). Use of Flumes in Measuring Discharge. Techniques of Water-Resources Investigations of the U.S. Geological Survey, Book 3, Chapter A14.
- Parshall, R. L. (1928). The Improved Venturi Flume. Bulletin No. 336, Agricultural Experiment Station, Colorado Agricultural College, Fort Collins, CO.
- Robinson, A. R. (1959). Report on Trapezoidal Measuring Flumes for Determining Discharge in Steep Ephemeral Streams. Colorado Agricultural and Mechanical College, Rocky Mountain Forest and Range Experimental Station, Report CER59AAR1, 13 p.
- Ruth, B. C. (1997). The Effects of Settlement on Cutthroat Flume Accuracy. M.S. Thesis, Colorado State University, Department of Civil Engineering, Fort Collins, CO.
- Skogerboe, G. V. and Hyatt, M. L. (1967). Analysis of Submergence in Flow Measuring Flumes. *J. Hydraulics Division*, ASCE, 93(HY4).
- Smith, R. E. *et al.* (1981). Supercritical Flow Flumes for Measuring Sediment-laden Flow. Department of Agriculture, Technical Bulletin Number 1655.

U.S. Bureau of Reclamation (1953, Revised 1984). Water Measurement Manual. United States Department of the Interior, Denver, CO.

Van Haveren, B.P. (1986). Water Resource Measurements. American Water Works Association, 132 p.

APPENDIX A – EXPANDED DATA TABLES

Table A.1: Expanded Version of Table 4.6

6-inch Parshall Flume Roughness Type I						
4% Slope		5% Slope		7% Slope		
Supercritical Regime		Supercritical Regime		Supercritical Regime	Supercritical Regime	Supercritical Regime
$Q = 10.15h_a^{1.28}$		$Q = 12.00h_a^{1.30}$		$Q = 11.38h_a^{1.28}$	Average	Standard Deviation
h_a	Q	Q	Q	Q	σ	Percent Difference
(ft)	(ft³/s)	(ft³/s)	(ft³/s)	(ft³/s)		
0.15	0.90	1.02	1.00	0.97	0.07	6.94
0.20	1.29	1.48	1.45	1.41	0.10	7.14
0.25	1.72	1.98	1.93	1.88	0.14	7.30
0.30	2.17	2.51	2.44	2.37	0.18	7.43
0.35	2.65	3.07	2.97	2.89	0.22	7.55
0.40	3.14	3.65	3.52	3.44	0.26	7.66
0.45	3.65	4.25	4.10	4.00	0.31	7.75
0.50	4.18	N/A	N/A	N/A	N/A	N/A

N/A = not applicable

Table A.2: Expanded Version of Table 4.9

9-inch Parshall Flume Roughness Type II						
4% Slope		5% Slope		7% Slope		
Subcritical Regime		Subcritical Regime		Subcritical Regime	Subcritical Regime	Subcritical Regime
$Q = 3.31h_a^{1.19}$		$Q = 3.16h_a^{1.23}$		$Q = 3.00h_a^{1.14}$	Average	Standard Deviation
h_a	Q	Q	Q	Q	σ	Percent Difference
(ft)	(ft³/s)	(ft³/s)	(ft³/s)	(ft³/s)		
0.40	1.11	1.02	1.06	1.06	0.04	4.22
0.45	1.28	1.18	1.21	1.22	0.05	4.10
0.50	1.45	1.35	1.36	1.39	0.06	4.05
0.55	1.63	1.51	1.52	1.55	0.06	4.05
0.60	1.80	1.69	N/A	N/A	N/A	N/A
0.65	1.98	1.86	N/A	N/A	N/A	N/A
0.70	2.17	2.04	N/A	N/A	N/A	N/A
0.75	2.35	2.22	N/A	N/A	N/A	N/A
0.80	2.54	2.40	N/A	N/A	N/A	N/A
0.85	2.73	2.59	N/A	N/A	N/A	N/A
0.90	2.92	2.78	N/A	N/A	N/A	N/A
0.95	3.11	2.97	N/A	N/A	N/A	N/A
1.00	3.31	3.16	N/A	N/A	N/A	N/A
1.05	3.51	3.36	N/A	N/A	N/A	N/A
1.10	3.71	3.55	N/A	N/A	N/A	N/A
1.15	3.91	3.75	N/A	N/A	N/A	N/A
1.20	4.11	3.95	N/A	N/A	N/A	N/A

N/A = not applicable

Table A.3: Expanded Version of Table 4.10

9-inch Parshall Flume Roughness Type III						
4% Slope		5% Slope		7% Slope		
Subcritical Regime		Subcritical Regime		Subcritical Regime		Subcritical Regime
$Q = 3.09h_a^{1.24}$		$Q = 3.35h_a^{1.21}$		$Q = 3.56h_a^{1.26}$		
h_a (ft)	Q (ft³/s)	Q (ft³/s)	Q (ft³/s)	Average Q (ft³/s)	Standard Deviation σ	Percent Difference
0.40	0.99	1.11	1.12	1.07	0.07	6.60
0.45	1.15	1.27	1.30	1.24	0.08	6.61
0.50	1.31	1.45	1.49	1.41	0.09	6.63
0.55	1.47	1.63	1.68	1.59	0.11	6.66
0.60	1.64	1.81	1.87	1.77	0.12	6.70
0.65	1.81	1.99	2.07	1.96	0.13	6.74
0.70	1.99	2.18	2.27	2.14	0.15	6.78
0.75	2.16	2.37	2.48	2.34	0.16	6.83
0.80	2.34	2.56	2.69	2.53	0.17	6.87
0.85	2.53	2.75	2.90	2.73	0.19	6.92
0.90	2.71	2.95	3.12	2.93	0.20	6.97
0.95	2.90	3.15	3.34	3.13	0.22	7.02
1.00	3.09	3.35	3.56	3.33	0.24	7.06
1.05	3.28	3.55	3.79	3.54	0.25	7.11
1.10	3.48	3.76	4.01	3.75	0.27	7.16
1.15	3.67	3.97	4.25	3.96	0.29	7.20
1.20	3.87	4.18	N/A	N/A	N/A	N/A

N/A = not applicable

Table A.4: Six-inch Parshall Flume 4% Slope – Variation in Roughness

6-inch Parshall Flume 4% Slope					
Roughness Type I		Roughness Type II			
Supercritical Regime		Subcritical Regime		Combined Regime	Combined Regime
$Q = 10.15h_a^{1.28}$		$Q = 2.26h_a^{1.13}$		Average	Standard Deviation
h_a (ft)	Q (ft³/s)	Q (ft³/s)	Q (ft³/s)	σ	Percent Difference
0.25	1.72	N/A	N/A	N/A	N/A
0.30	2.17	N/A	N/A	N/A	N/A
0.35	2.65	N/A	N/A	N/A	N/A
0.40	3.14	N/A	N/A	N/A	N/A
0.45	3.65	N/A	N/A	N/A	N/A
0.50	4.18	1.03	2.61	2.23	85.39
0.55	N/A	1.15	N/A	N/A	N/A
0.60	N/A	1.27	N/A	N/A	N/A
0.65	N/A	1.39	N/A	N/A	N/A
0.70	N/A	1.51	N/A	N/A	N/A
0.75	N/A	1.63	N/A	N/A	N/A
0.80	N/A	1.76	N/A	N/A	N/A
0.85	N/A	1.88	N/A	N/A	N/A
0.90	N/A	2.01	N/A	N/A	N/A
0.95	N/A	2.13	N/A	N/A	N/A
1.00	N/A	2.26	N/A	N/A	N/A
1.05	N/A	2.39	N/A	N/A	N/A

N/A = not applicable

Table A.5: Six-inch Parshall Flume 5% Slope – Variation in Roughness

6-inch Parshall Flume 5% Slope					
Roughness Type I		Roughness Type II			
Supercritical Regime		Subcritical Regime		Combined Regime	Combined Regime
$Q = 12.00h_a^{1.30}$		$Q = 2.32h_a^{1.12}$		Average	Standard
h_a (ft)	Q (ft³/s)	Q (ft³/s)	Q (ft³/s)	Q (ft³/s)	Deviation σ
					Percent Difference
0.15	1.02	N/A	N/A	N/A	N/A
0.20	1.48	N/A	N/A	N/A	N/A
0.25	1.98	N/A	N/A	N/A	N/A
0.30	2.51	N/A	N/A	N/A	N/A
0.35	3.07	N/A	N/A	N/A	N/A
0.40	3.65	N/A	N/A	N/A	N/A
0.45	4.25	N/A	N/A	N/A	N/A
0.50	N/A	1.07	N/A	N/A	N/A
0.55	N/A	1.19	N/A	N/A	N/A
0.60	N/A	1.31	N/A	N/A	N/A
0.65	N/A	1.43	N/A	N/A	N/A
0.70	N/A	1.56	N/A	N/A	N/A
0.75	N/A	1.68	N/A	N/A	N/A
0.80	N/A	1.81	N/A	N/A	N/A
0.85	N/A	1.93	N/A	N/A	N/A
0.90	N/A	2.06	N/A	N/A	N/A
0.95	N/A	2.19	N/A	N/A	N/A
1.00	N/A	2.32	N/A	N/A	N/A
1.05	N/A	2.45	N/A	N/A	N/A

N/A = not applicable

Table A.6: Six-inch Parshall Flume 7% Slope – Variation in Roughness

6-inch Parshall Flume 7% Slope					
Roughness Type I		Roughness Type II			
Supercritical Regime		Subcritical Regime		Combined Regime	Combined Regime
$Q = 11.38h_a^{1.28}$		$Q = 2.27h_a^{1.19}$		Average	Standard
h_a (ft)	Q (ft³/s)	Q (ft³/s)	Q (ft³/s)	Q (ft³/s)	Deviation σ
					Percent Difference
0.15	1.00	N/A	N/A	N/A	N/A
0.20	1.45	N/A	N/A	N/A	N/A
0.25	1.93	N/A	N/A	N/A	N/A
0.30	2.44	N/A	N/A	N/A	N/A
0.35	2.97	N/A	N/A	N/A	N/A
0.40	3.52	N/A	N/A	N/A	N/A
0.45	4.10	N/A	N/A	N/A	N/A
0.50	N/A	0.99	N/A	N/A	N/A
0.55	N/A	1.11	N/A	N/A	N/A
0.60	N/A	1.24	N/A	N/A	N/A
0.65	N/A	1.36	N/A	N/A	N/A
0.70	N/A	1.48	N/A	N/A	N/A
0.75	N/A	1.61	N/A	N/A	N/A
0.80	N/A	1.74	N/A	N/A	N/A
0.85	N/A	1.87	N/A	N/A	N/A
0.90	N/A	2.00	N/A	N/A	N/A
0.95	N/A	2.14	N/A	N/A	N/A
1.00	N/A	2.27	N/A	N/A	N/A
1.05	N/A	2.41	N/A	N/A	N/A

N/A = not applicable

Table A.7: Expanded Version of Table 4.11

9-inch Parshall Flume 4% Slope									
	Roughness Type I	Roughness Type II	Roughness Type III						
	Supercritical Regime	Subcritical Regime	Subcritical Regime	Subcritical Regime	Subcritical Regime	Subcritical Regime	Combined Regime	Combined Regime	Combined Regime
	$Q = 10.93h_a^{1.27}$	$Q = 3.31h_a^{1.19}$	$Q = 3.09h_a^{1.24}$	Average	Standard Deviation	Percent Difference	Average	Standard Deviation	Percent Difference
h_a (ft)	Q (ft ³ /s)	σ		Q (ft ³ /s)	σ				
0.15	0.98	N/A	N/A	N/A	N/A	N/A	N/A	N/A	N/A
0.20	1.42	N/A	N/A	N/A	N/A	N/A	N/A	N/A	N/A
0.25	1.88	N/A	N/A	N/A	N/A	N/A	N/A	N/A	N/A
0.30	2.37	N/A	N/A	N/A	N/A	N/A	N/A	N/A	N/A
0.35	2.88	N/A	N/A	N/A	N/A	N/A	N/A	N/A	N/A
0.40	3.41	1.11	0.99	1.05	0.09	8.09	1.84	1.36	74.20
0.45	3.96	1.28	1.15	1.21	0.09	7.68	2.13	1.59	74.60
0.50	N/A	1.45	1.31	1.38	0.10	7.31	N/A	N/A	N/A
0.55	N/A	1.63	1.47	1.55	0.11	6.97	N/A	N/A	N/A
0.60	N/A	1.80	1.64	1.72	0.11	6.66	N/A	N/A	N/A
0.65	N/A	1.98	1.81	1.90	0.12	6.38	N/A	N/A	N/A
0.70	N/A	2.17	1.99	2.08	0.13	6.12	N/A	N/A	N/A
0.75	N/A	2.35	2.16	2.26	0.13	5.88	N/A	N/A	N/A
0.80	N/A	2.54	2.34	2.44	0.14	5.65	N/A	N/A	N/A
0.85	N/A	2.73	2.53	2.63	0.14	5.44	N/A	N/A	N/A
0.90	N/A	2.92	2.71	2.82	0.15	5.23	N/A	N/A	N/A
0.95	N/A	3.11	2.90	3.01	0.15	5.04	N/A	N/A	N/A
1.00	N/A	3.31	3.09	3.20	0.16	4.86	N/A	N/A	N/A
1.05	N/A	3.51	3.28	3.40	0.16	4.69	N/A	N/A	N/A
1.10	N/A	3.71	3.48	3.59	0.16	4.52	N/A	N/A	N/A
1.15	N/A	3.91	3.67	3.79	0.17	4.37	N/A	N/A	N/A
1.20	N/A	4.11	3.87	3.99	0.17	4.22	N/A	N/A	N/A

N/A = not applicable

Table A.8: Expanded Version of Table 4.12

9-inch Parshall Flume 5% Slope									
	Roughness Type I	Roughness Type II	Roughness Type III						
	Supercritical Regime	Subcritical Regime	Subcritical Regime	Subcritical Regime	Subcritical Regime	Subcritical Regime	Combined Regime	Combined Regime	Combined Regime
	$Q = 8.79h_a^{1.04}$	$Q = 3.16h_a^{1.23}$	$Q = 3.35h_a^{1.21}$	Average	Standard Deviation	Percent Difference	Average	Standard Deviation	Percent Difference
h_a (ft)	Q (ft ³ /s)	σ		Q (ft ³ /s)	σ				
0.15	1.22	N/A	N/A	N/A	N/A	N/A	N/A	N/A	N/A
0.20	1.65	N/A	N/A	N/A	N/A	N/A	N/A	N/A	N/A
0.25	2.08	N/A	N/A	N/A	N/A	N/A	N/A	N/A	N/A
0.30	2.51	N/A	N/A	N/A	N/A	N/A	N/A	N/A	N/A
0.35	2.95	N/A	N/A	N/A	N/A	N/A	N/A	N/A	N/A
0.40	3.39	1.02	1.11	1.06	0.06	5.42	1.84	1.34	73.00
0.45	3.83	1.18	1.27	1.23	0.06	5.26	2.10	1.50	71.69
0.50	N/A	1.35	1.45	1.40	0.07	5.11	N/A	N/A	N/A
0.55	N/A	1.51	1.63	1.57	0.08	4.97	N/A	N/A	N/A
0.60	N/A	1.69	1.81	1.75	0.08	4.85	N/A	N/A	N/A
0.65	N/A	1.86	1.99	1.92	0.09	4.74	N/A	N/A	N/A
0.70	N/A	2.04	2.18	2.11	0.10	4.63	N/A	N/A	N/A
0.75	N/A	2.22	2.37	2.29	0.10	4.53	N/A	N/A	N/A
0.80	N/A	2.40	2.56	2.48	0.11	4.44	N/A	N/A	N/A
0.85	N/A	2.59	2.75	2.67	0.12	4.36	N/A	N/A	N/A
0.90	N/A	2.78	2.95	2.86	0.12	4.28	N/A	N/A	N/A
0.95	N/A	2.97	3.15	3.06	0.13	4.20	N/A	N/A	N/A
1.00	N/A	3.16	3.35	3.26	0.13	4.13	N/A	N/A	N/A
1.05	N/A	3.36	3.55	3.45	0.14	4.06	N/A	N/A	N/A
1.10	N/A	3.55	3.76	3.66	0.15	3.99	N/A	N/A	N/A
1.15	N/A	3.75	3.97	3.86	0.15	3.93	N/A	N/A	N/A
1.20	N/A	3.95	4.18	4.07	0.16	3.87	N/A	N/A	N/A

N/A = not applicable

Table A.9: Expanded Version of Table 4.13

9-inch Parshall Flume 7% Slope													
Roughness Type I	Roughness Type II	Roughness Type II	Roughness Type III										
Super-critical Regime	Super-critical Regime	Sub-critical Regime	Sub-critical Regime	Super-critical Regime	Super-critical Regime	Super-critical Regime	Sub-critical Regime	Sub-critical Regime	Sub-critical Regime	Sub-critical Regime	Com-bined Regime	Com-bined Regime	Com-bined Regime
$Q = 11.37h_a^{1.22}$	$Q = 11.34h_a^{1.33}$	$Q = 3.00h_a^{1.14}$	$Q = 3.56h_a^{1.26}$	Average Q (ft ³ /s)	Standard Deviation σ	Percent Difference	Average Q (ft ³ /s)	Standard Deviation σ	Percent Difference	Average Q (ft ³ /s)	Standard Deviation σ	Percent Difference	
h_a (ft)	Q (ft ³ /s)	Q (ft ³ /s)	σ	Q (ft ³ /s)	σ	Q (ft ³ /s)	σ	Q (ft ³ /s)	σ	Q (ft ³ /s)			
0.15	1.12	N/A	N/A	N/A	N/A	N/A	N/A	N/A	N/A	N/A	N/A	N/A	N/A
0.20	1.60	N/A	N/A	N/A	N/A	N/A	N/A	N/A	N/A	N/A	N/A	N/A	N/A
0.25	2.10	1.79	N/A	N/A	1.94	0.21	10.95	N/A	N/A	N/A	N/A	N/A	N/A
0.30	2.62	2.29	N/A	N/A	2.45	0.23	9.54	N/A	N/A	N/A	N/A	N/A	N/A
0.35	3.16	2.81	N/A	N/A	2.98	0.25	8.34	N/A	N/A	N/A	N/A	N/A	N/A
0.40	3.72	3.35	1.06	1.12	3.54	0.26	7.31	1.09	0.05	4.33	2.31	1.42	61.44
0.45	4.29	3.92	1.21	1.30	4.11	0.26	6.39	1.25	0.07	5.32	2.68	1.65	61.71
0.50	N/A	N/A	1.36	1.49	N/A	N/A	N/A	1.42	0.09	6.22	N/A	N/A	N/A
0.55	N/A	N/A	1.52	1.68	N/A	N/A	N/A	1.60	0.11	7.02	N/A	N/A	N/A
0.60	N/A	N/A	N/A	1.87	N/A	N/A	N/A	N/A	N/A	N/A	N/A	N/A	N/A
0.65	N/A	N/A	N/A	2.07	N/A	N/A	N/A	N/A	N/A	N/A	N/A	N/A	N/A
0.70	N/A	N/A	N/A	2.27	N/A	N/A	N/A	N/A	N/A	N/A	N/A	N/A	N/A
0.75	N/A	N/A	N/A	2.48	N/A	N/A	N/A	N/A	N/A	N/A	N/A	N/A	N/A
0.80	N/A	N/A	N/A	2.69	N/A	N/A	N/A	N/A	N/A	N/A	N/A	N/A	N/A
0.85	N/A	N/A	N/A	2.90	N/A	N/A	N/A	N/A	N/A	N/A	N/A	N/A	N/A
0.90	N/A	N/A	N/A	3.12	N/A	N/A	N/A	N/A	N/A	N/A	N/A	N/A	N/A
0.95	N/A	N/A	N/A	3.34	N/A	N/A	N/A	N/A	N/A	N/A	N/A	N/A	N/A
1.00	N/A	N/A	N/A	3.56	N/A	N/A	N/A	N/A	N/A	N/A	N/A	N/A	N/A
1.05	N/A	N/A	N/A	3.79	N/A	N/A	N/A	N/A	N/A	N/A	N/A	N/A	N/A
1.10	N/A	N/A	N/A	4.01	N/A	N/A	N/A	N/A	N/A	N/A	N/A	N/A	N/A
1.15	N/A	N/A	N/A	4.25	N/A	N/A	N/A	N/A	N/A	N/A	N/A	N/A	N/A

N/A = not applicable